

# OPTIMAL FEES FOR LIQUIDITY PROVISION IN AUTOMATED MARKET MAKERS

STEVEN CAMPBELL, PHILIPPE BERGAULT, JASON MILIONIS, AND MARCEL NUTZ

**ABSTRACT.** Passive liquidity providers (LPs) in automated market makers (AMMs) face losses due to adverse selection (LVR), which static trading fees often fail to offset in practice. We study the key determinants of LP profitability in a dynamic reduced-form model where an AMM operates in parallel with a centralized exchange (CEX), traders route their orders optimally to the venue offering the better price, and arbitrageurs exploit price discrepancies. Using large-scale simulations and real market data, we analyze how LP profits vary with market conditions such as volatility and trading volume, and characterize the optimal AMM fee as a function of these conditions. We highlight the mechanisms driving these relationships through extensive comparative statics, and confirm the model’s relevance through market data calibration. A key trade-off emerges: fees must be low enough to attract volume, yet high enough to earn sufficient revenues and mitigate arbitrage losses. We find that under normal market conditions, the optimal AMM fee is competitive with the trading cost on the CEX and remarkably stable, whereas in periods of very high volatility, a high fee protects passive LPs from severe losses. These findings suggest that a threshold-type dynamic fee schedule is both robust enough to market conditions and improves LP outcomes.

## 1. INTRODUCTION

Decentralized exchanges (DEXs) are an important class of trading venues in decentralized finance (DeFi), allowing users to trade assets or provide liquidity without intermediation. Most DEXs operate using automated market makers (AMMs) where traders interact with a liquidity pool rather than being matched directly as in a limit order book.<sup>1</sup> Exchange rates are set by predetermined formulas, most often following the constant function market maker (CFMM) model which enforces a fixed relationship between asset quantities in the pool. A key attraction of CFMMs is *passive* liquidity provision—liquidity providers (LPs) can supply liquidity without managing their positions continuously as in limit order book markets. In return for providing liquidity, LPs earn a pro-rata share of fees that are levied on trades in the AMM. However, the convenience of not managing positions comes at a cost: LPs are exposed to losses due to adverse selection (see Capponi and Jia [13] and Milionis et al. [31], among others). Indeed, rational market participants monitoring real-time prices on other venues where price discovery occurs can exploit stale prices offered by the AMM. Even after hedging away price risk, LPs incur a systematic loss known as loss-versus-rebalancing (LVR, see Milionis et al. [31], also identified as “convexity cost,” see Cartea et al. [14, 15]). While fees would ideally compensate for that, practice has shown that LPs often suffer persistent negative returns, especially in volatile markets (e.g., [11, 17, 18]). This poses a serious challenge to the long-term sustainability of passive liquidity

---

*Date:* August 12, 2025.

<sup>1</sup>See <https://defillama.com/dexs> for up-to-date trading volume statistics. We lightly abuse terminology in using the terms DEX and AMM interchangeably.

provision (e.g., Hasbrouck et al. [23]). Therefore, a plurality of recent works study this issue and possible solutions from various angles, such as dynamic fees adjusting to volatility (Cao et al. [12]), modifications to blockchain frequency (Milionis et al. [30]), or auction-based AMM designs redistributing arbitrage gains to LPs (Adams et al. [1]), among many others. The practical relevance of such approaches is also evidenced by the numerous works from industry groups aiming to mitigate LVR (e.g., [3, 16, 20, 26, 27]). Despite this rapidly growing body of literature, a simulation-based, model-agnostic framework for analyzing LP profitability is absent.

The goal of the present work is to understand the PnL of passive liquidity provision *as a function of market conditions* such as trading fees, price volatility, and trading volume. In particular, we want to determine the AMM fee that maximizes expected LP PnL given market conditions, and whether that PnL is positive. Moreover, we want to understand how much the PnL deteriorates when the AMM fee deviates from the optimum, perhaps because market conditions evolve over time. One motivation for the present work is the proposal of *dynamic fees* (that vary as a function of market conditions) as a way to reduce LVR. In the context of Uniswap v4 hook design, Uniswap’s guidance highlights volatility and trade volume dependence as a best practice in fee design [32].

In contrast to the existing related literature (see Section 1.3 for a literature review), we propose a reduced-form model where the market conditions are *input* parameters—rather than an equilibrium model which endogenizes some or all of the conditions. Using large-scale simulation, we can then explore the hypersurface of all parameter combinations. A dynamic market where conditions evolve jointly over time can be seen as a curve traveling on that hypersurface, so that our study can inform LP profitability in a dynamic situation: a simulation with constant parameters over a short time horizon serves as a building block of a dynamic model obtained by concatenating several simulations with different parameters. While the evolution would certainly include market and asset-specific dynamics, the design of the building block is agnostic to those.

**1.1. Model.** In our baseline model, the numéraire asset  $X$  and the risky asset  $Y$  are traded on two venues, a centralized exchange (CEX) and a decentralized exchange operating by an AMM, more precisely a constant product market maker (first analyzed by Angeris et al. [4]) akin to Uniswap v2.<sup>2</sup> The price of  $Y$  (in units of  $X$ ) on the CEX evolves exogenously and the assets can be traded at a fixed proportional cost  $\eta^0$  which stands in for all trading costs on the CEX—nominal fees levied by the exchange, bid-ask spread, etc. The liquidity for the AMM is supplied by a representative LP at the initial time. After that, no shares are minted or burnt, so that pool reserves on the AMM evolve only due to swaps by traders. Swaps on the AMM incur a proportional fee  $\eta^1$  which is paid to the LP. There are two types of traders. *Arbitrageurs* act whenever prices on the two venues allow for a profitable roundtrip after accounting for fees. Their trades thus align the marginal price on the AMM with the CEX price, up to fees. Traders of the second type are called *fundamental traders* and differ only by having an exogenous trading demand. To satisfy their demand, they route their order flow optimally to the two venues, meaning that each marginal trade is routed to the

---

<sup>2</sup>While Uniswap v3 with concentrated liquidity carries higher trading volume at the time of writing, and v4 with hooks is the most recent Uniswap protocol, we prefer a parsimonious model with few parameters to study the mechanics of CEX-DEX interaction. In such a model, producing realistic price ratios is a nontrivial sanity check (see Section 5), whereas with a very large parameter set as in v3 (even infinite in v4), it would be difficult to draw any conclusions.

venue offering a better marginal price after fees.<sup>3</sup> As a result, some of the fundamental flow may go to the AMM and contribute to aligning the price with the CEX, even when there is no profitable roundtrip. We evaluate the expected PnL of the representative LP, which comprises the fees accrued plus the change in marked-to-CEX value of the pool reserves.

Before moving on to our results, let us pause to highlight how our setup differs from the existing literature studying the interaction of an AMM with a CEX (see also Section 1.3). Most previous works assume that the CEX is frictionless—while trading on the AMM is subject to a fee, trading on the CEX does not incur any fee or slippage. Then, trading on the AMM should be attractive only to one side of the informed market; for instance, buyers if the price on the AMM, inclusive of fee, is lower than the CEX price. The resulting trades would be the ones with the highest adverse selection cost to LPs, and it is intuitive that liquidity provision would never be beneficial in this situation. Previous works include noise traders who trade on the AMM *regardless* of prices on the CEX. This adds trades that are on average profitable to LPs as soon as the AMM fee is positive, so that a sufficiently large volume of noise trades renders liquidity provision profitable. By contrast, our baseline model does not have noise traders. While our fundamental traders have an exogenous trading motive, they are informed about CEX prices and route their flow optimally between the two venues.

In the absence of noise traders, a key reason that liquidity provision can be profitable is that trading on the CEX *is not free either*. Indeed, both venues offer a combination of price and slippage. Even when the AMM marginal price is inferior to the CEX price, the AMM can be competitive for fundamental flow if its fee is lower. Specifically, a marginal fundamental buyer prefers the AMM if AMM marginal price plus AMM fee is lower than CEX price plus CEX fee. For an LP who marks assets to CEX prices and earns the AMM fee, this means that the trade is potentially profitable.<sup>4</sup>

In the absence of free money from noise traders, the AMM needs to compete with the CEX in terms of trading costs. This idea will be underscored by our quantitative results on optimal AMM fees below, which will show that the AMM can make up for its stale pricing by offering a competitive fee, and carve out a regime where LP provision is profitable without noise traders. This is a conservative assessment: We agree with the literature that in reality there are traders who will avoid the CEX even when its price is more attractive, for instance, to avoid counterparty risk or Know Your Customer regulations. Adding noise traders to our model as a third type of trader will only increase LP profitability, as is discussed in Section 6 among other extensions of our baseline model.

**1.2. Contributions and Results.** Before discussing the insights derived from our model, let us briefly highlight the implementation itself. To meet the computational demands of large-scale experimentation, we provide an efficient, parallelized code base ready to deploy on high-performance computing clusters. The implementation is modular and extensible, so that interested researchers can run their own experiments. The code is publicly available.<sup>5</sup>

Thanks to our reduced-form modeling approach, we can produce comparative statics with respect to any parameter, and that is key to our goal of understanding LP profitability.

---

<sup>3</sup>Equivalently, fundamental traders send all their orders to a smart router (aggregator) monitoring both venues.

<sup>4</sup>If the AMM price inclusive of fee exceeds the CEX price without fee, the difference will be the LP's marginal net profit (which is therefore bounded from above by the CEX fee). If not, the trade results in a loss for the LP.

<sup>5</sup><https://github.com/JasonSome/cpmm-trading/tree/master>

Assuming that the CEX price follows a driftless geometric Brownian motion,<sup>6</sup> the price dynamics are summarized by a single volatility parameter  $\sigma$ . In line with previous findings, our simulation shows that all else equal, expected LP PnL is decreasing in volatility. On the other hand, it is increasing in fundamental demand, which was not considered before.<sup>7</sup> We highlight the mechanics leading to those effects by extensively analyzing (a) the distribution of the ratio between AMM and CEX prices, which captures the adverse selection cost of trades, and (b) the volume attracted by the AMM, which multiplies the gross PnL of those trades and additionally the LP’s fee earnings. Greater CEX price volatility is reflected in wider dispersion of the price ratio distribution, thus increasing adverse selection and reducing PnL. Increasing fundamental demand generally means that the AMM captures more volume, increasing fee revenue. More importantly, this additional fundamental flow tends to trade at prices that imply smaller adverse selection costs or even profits (depending on the relationship between AMM and CEX fees): When CEX prices sufficiently deviate from AMM prices, the AMM attracts one-sided fundamental flow (only buyers or only sellers) which acts as a *reverting drift* on the price ratio process even before arbitrage opportunities arise.<sup>8</sup> This effect is clearly seen in the narrowing price ratio distribution, and exemplifies how volatility and fundamental demand tend to act in opposition in shaping the ratio distribution. Such an effect has not been observed in previous works.

While our reduced form model allows us to discuss comparative statics individually for each parameter, it is important to remember that market characteristics are likely correlated in practice. For instance, our simulation also shows that if a volatility increase is accompanied by a surge in demand, the net effect on LP PnL can be approximately flat. However, all else fixed, a sufficiently large volatility will always render liquidity provision unprofitable: in the limit  $\sigma \rightarrow \infty$ , both the arbitrage volume and the per-trade adverse selection loss tend to infinity. A detailed discussion of LP profitability and comparative statics can be found in Section 3.

Next, we highlight the complex role of the AMM fee, likely the most interesting parameter in light of the current discussions about AMM design. Higher fees increase per-trade revenues for the LP and defend against adverse selection. On the other hand, higher fees reduce the volume captured by the AMM, reducing fee income but also increasing price stickiness as the reverting force of fundamental flow is reduced and arbitrage requires greater price disparities. This economic narrative is central to our analysis: the LP cannot choose its fee in a vacuum; instead, fee-setting happens in direct competition with the CEX, and every basis-point change carries downstream consequences for trade volume, price action, revenue generation, and arbitrage activity.

For a broad range of volatility and fundamental demand parameters (which we interpret as normal market conditions), we find that there is a unique optimal AMM fee maximizing expected LP PnL. The optimal fee *undercuts* the representative CEX trading cost  $\eta^0$ , in line with the aforementioned idea that the AMM needs to be competitive with the CEX in terms of slippage. Indeed, slippage on the AMM is given by AMM fee plus price impact

---

<sup>6</sup>While we focus here on geometric Brownian motion, the simulation accepts any time series as input for the CEX price, be it a sample from a stochastic process or real-world price data as discussed in Section 5.

<sup>7</sup>PnL is also increasing in noise trader volume if such traders are included. This agrees with previous findings and is also straightforward analytically as fee income from noise trader volume amounts to a direct transfer to LPs.

<sup>8</sup>If prices deviate even more, the ratio process is *reflected* at the threshold where the arbitrage opportunity arises.

whereas slippage on the CEX is given by the CEX fee alone, hence undercutting by a modest amount is an intuitive choice for a competitive AMM fee. Nevertheless, it seems that we are the first to make this direct connection between optimal AMM fee and trading costs on the CEX.

At this point, it is important to remember that our CEX fee represents all trading costs on the CEX. While assuming a single representative number is useful for comparative statics and the empirical experiments below, we also note that in reality, different traders incur different costs when trading on a CEX, for instance because nominal fees differ by volume tiers<sup>9</sup> or because the slippage of a sophisticated execution algorithm is smaller than for a simple market order. On the other hand, the AMM fee is the same for all traders. Thus, in practice, the message of undercutting may be interpreted as offering a better fee for *some* traders, perhaps retail customers that form a relatively important fraction in cryptocurrency markets. See also the discussion in Section 6.3. In Section 5, the representative CEX fee is determined by *calibrating* to the price ratio distribution rather than using posted nominal fees.

Returning to the discussion of simulation results, the optimal AMM fee is increasing in volatility and decreasing in demand throughout the regime of normal markets, reflecting the changing tradeoff between volume capture and defending against adverse selection losses.<sup>10</sup> The sensitivity of the optimal fee, as well as the level itself, are significantly lower than in previous studies. While our optimal AMM fee is below the CEX fee, previous models implied optimal AMM fees at very elevated levels, for instance around 125–250 basis points (bps) for the volatility range presented in the recent work of He et al. [25, Figure 5]. While the methodology in previous works is quite different, it is intuitive that inclusion of fundamental traders generally lowers the optimal AMM fee. Our findings align with the recent popularity of 5 bps pools (see also Section 7).

Our simulation allows us to study in detail the PnL regret, i.e., how much PnL is diminished when the fee is not optimal. We find that in the regime of normal markets, and more generally as long as volatility does not exceed the threshold where liquidity provision becomes unprofitable, the regret is quite moderate when the AMM fee is kept at a well-chosen value below the CEX fee. This has important practical implications for AMM design, as discussed in Section 7.

When the volatility exceeds that threshold, the optimal fee ceases to exist: while the optimum is quite stable up to the threshold (hovering slightly below the CEX fee), the optimal fee is infinite above the threshold as the LP prefers to halt trading on the AMM. The precise threshold depends on the market parameters—if an increase in volatility is accompanied by a sufficiently large increase in fundamental trading volume, the optimal fee remains fairly stable. Our results on AMM fees are reported in Section 4, and some practical conclusions for a threshold-type dynamic fee schedule are in Section 7.

Our empirical analysis in Section 5 demonstrates that our stylized framework, despite its parsimony, captures relevant features of real-world markets. Because our simulation accommodates arbitrary price trajectories, we can feed observed CEX time series directly into the model for calibration and testing. Using high-frequency data for ETH/USDC from

---

<sup>9</sup>For instance, <https://www.binance.com/en/fee/schedule> lists a maker/taker fee of 10 basis points (bps) for users with a 30-day trading volume under \$1M, decreasing to 4/5.2 bps for a user with a \$100M volume (as of June 30, 2025).

<sup>10</sup>In a regime of small fundamental demand, the optimal fee is decreasing-then-increasing. An explanation can be found in Section 4.

Binance and Uniswap, we estimate the model’s three core parameters: the CEX fee, price volatility, and fundamental demand. With only these inputs, the model reproduces a price ratio distribution that closely aligns with empirical observations. The calibrated CEX fee converges near posted taker rates, and estimated volatility falls within plausible intraday ranges. Importantly, when testing LP performance on real price data, we find that lowering the AMM fee below the *effective* CEX level improves LP profitability—a conclusion that reinforces our simulation results and underscores the model’s practical relevance.

To confirm that our conclusions are robust, Section 6 considers several extensions of the baseline model. These extensions include adding noise traders that always prefer the AMM to the CEX, additional fee levels, changing trading frequency, and CEX prices with drift.

**1.3. Related Literature.** The interaction between an AMM and a CEX, and the resulting adverse selection on the AMM, have been studied in a number of papers. Capponi and Jia [13] consider a group of LPs that maximize expected profits by controlling the amount of liquidity they provide in a one-period model. The authors observe that LPs in CFMMs suffer losses when risky asset prices move, and calculate the welfare-maximizing convexity of the CFMM invariant, trading off losses from arbitrage with increased price impact of investors. Lehar and Parlour [28] show theoretically and empirically that the equilibrium pool size is smaller when asset volatility is higher and larger when noise trading volume is higher, and characterize a number of other stylized facts of Uniswap liquidity pools. Hasbrouck et al. [24] show that when a group of LPs can choose between providing liquidity and an outside investment, a higher unit trading fee on the AMM can increase equilibrium liquidity provision and trading volume on the AMM, due to decreasing price impact.

Closest to our model in terms of order flow routing is the work of Aoyagi and Ito [5] which examines the amount of liquidity in a one-period equilibrium model where LPs factor in opportunity cost. The main similarity with our modeling is that in addition to noise traders, there are informed traders choosing between the AMM and CEX depending on prices, bid-ask spread on CEX and fee on AMM. However, in their model, informed traders always cause a *loss* to LPs (and noise traders always cause a gain, see Lemmas 5 and 6 in [5]). The equilibrium amount of liquidity provision is found to be hump-shaped in volatility. Moreover, there is a positive spillover effect between liquidity on AMM and CEX, contrary to the centralization phenomenon usually observed between venues of the same type. Like most equilibrium models, [5] does not aim to (and is unable to) investigate LP profitability; indeed, the equilibrium is determined by *imposing* the break-even condition that expected LP PnL equals *zero*.

Closest in terms of goal, namely studying optimal AMM fees when competing with a CEX, is the work of He et al. [25]. In a dynamic model where CEX prices are exogenous and arbitrageurs adjust prices on the AMM while noise traders ignore price differences, LPs are risk-averse and optimize dynamically between liquidity provision in the AMM and investment in the CEX. (Here, LPs are active—the amount of liquidity provided responds to every CEX price increment, with no gas fees.) Among other questions, the authors study the optimal fee level on the AMM. Assuming stationary distribution of the state variables, LPs’ expected utility is numerically found to be increasing-then-decreasing with respect to the fee, and the optimal fee is increasing with respect to volatility. Qualitatively, this is in line with our results in Section 4. Quantitatively, the optimal AMM fee is reported at 125–250 bps for a range of volatilities, but we note that numerical values may ultimately

be driven by assumptions on risk aversion coefficients and sharp ratios that are difficult to pin down in practice. No such assumptions are needed in our risk-neutral model.

In terms of approach, the present work is complementary to the above. While equilibrium and utility-maximization approaches can give valuable insights into interactions, the present reduced-form approach is more directly applicable by practitioners. As shown in Section 5, real-world time series can be used for asset prices and latent parameters can be calibrated to observables such as asset price ratios. While we cannot hope to infer equilibrium reactions, we can observe realistic patterns of order flow and LP PnL at existing market conditions.

As mentioned, dynamic AMM fees (that vary with market conditions) have been proposed to reduce LVR and are one motivation for the present study. There are existing protocols that leverage dynamic fees in an empirical manner to provide liquidity providers with better arbitrage protection (e.g., LFJ [29] and Elsts [19]), including in the context of Uniswap v4 hook design, but they are mostly using ad-hoc solutions based on real-time empirics. For instance, LFJ [29] implements the variable fee as a quadratic function of instantaneous volatility. Attempts to understand the benefits of dynamic fees have appeared in the work of Cao et al. [12] who conduct an optimization over volatility-dependent fees in a static single-period model *without* CEX competition. More similar to the present work, Volosnikov et al. [33] study profitability depending on fixed or sigmoid volatility-dependent fees by simulation, but again without taking competition by a CEX into account. Fritsch [21] studies fees in a static Nash equilibrium between competing AMMs, also without a CEX. The systematic study of fees as a function of market conditions in a competitive setting is a crucial gap in the literature that is addressed by our work.

A different stream of literature studies potential AMM designs with a price oracle, essentially meaning that the CEX price is a state variable of the AMM. Bergault et al. [8] use a mean-variance framework inspired by portfolio theory to investigate the use of non-adversarial quotes for AMMs and perform simulations under various market conditions; see also [9, 10] for extensions. Aqsha et al. [6] use a principal-agent framework to study the optimal mechanism to redistribute a CFMM’s fixed fee to LPs in order to maximize order flow. Most recently, Baggiani et al. [7] study optimal dynamic fees in a CFMM using stochastic control. We emphasize that the present setting is fundamentally different as the adverse selection issue is directly related to the latency in price discovery which would be removed by the oracle.<sup>11</sup>

There is by now a substantial literature on AMMs, in addition to the classical literature on market microstructure. For a more extensive review, see for instance He et al. [25, Section 1.1].

**1.4. Organization.** The remainder of this paper is structured as follows. Section 2 describes the market model consisting of CEX, DEX, traders, and LP, together with the sequence of their interactions. Section 3 investigates how market characteristics affect LP returns and highlights the underlying mechanisms by analyzing the price ratio and volume distributions. Section 4 focuses on the optimal fee for LPs and its robustness. Section 5 contains the empirical analysis applying our model to Binance and Uniswap data. Section 6 confirms that our main findings are robust to several extensions of the model. Section 7

---

<sup>11</sup>For example, when (as in [7]) there are two dynamic fees (for buying and selling) and both can depend on the CEX price, then one possible fee schedule is to make AMM prices (inclusive of fees) equal to CEX prices, eliminating adverse selection.

concludes. Appendix A gives pseudo-code for the simulation algorithm. Appendix B details various summary statistics for the simulations with different parameters underlying the price ratio histograms shown in Figure 6 of Section 3. Appendix C reports an analytical derivation for a limiting regime of large demand and small volatility that is discussed Section 4.

## 2. THE MODEL

We propose a stylized model of an economy with two assets and two trading venues. The first asset, denoted  $X$ , serves as a reference currency or *numéraire*. The second asset, denoted  $Y$ , plays the role of the risky asset. In our examples, we take  $X$  to be the stablecoin USDC and  $Y$  to be ETH. The two assets are traded against one another on a centralized exchange (CEX) and a decentralized exchange (DEX). Trading evolves over a time interval  $[0, T]$  and is simulated as  $N$  discrete periods of equal length  $\delta t = T/N$ . There will be three types of agents: arbitrageurs, fundamental traders, and liquidity providers. (Section 6 additionally considers noise traders.) Below, we first detail each of these ingredients, then explain how they interact in the simulation.

*CEX.* The price  $S_t^0$  of the risky asset  $Y$  at time  $t$  (denominated in units of  $X$ ) on the CEX follows exogenous dynamics. Most of our exposition uses a simulated price, namely, a geometric Brownian motion with zero drift:  $S_t^0$  has continuous dynamics

$$(2.1) \quad \log(S_t^0/S_0^0) = -\frac{1}{2}\sigma^2 t + \sigma W_t, \quad t \geq 0,$$

where  $W = (W_t)_{t \geq 0}$  is a standard Brownian motion, and this process is sampled at the discrete trading periods. We choose this model for simplicity and parsimony. That said, our implementation can accept an arbitrary time series as input for  $S_t^0$ , and Section 5 presents an empirical analysis where  $S_t^0$  follows a historical time series from Binance instead of a simulated price. Section 6 considers simulated processes with drift.

As we are modeling a situation where the CEX is a highly liquid trading venue (relative to the DEX), trading on the CEX incurs a proportional fee  $\eta^0 > 0$ , but no price impact. We emphasize that this fee stands in for *all trading costs* on the CEX (such as bid-ask spread for market orders, adverse selection costs for limit orders, etc.), thus may be larger than the nominal fee posted on exchanges like Binance. The role of  $\eta^0$  will be highlighted in greater detail below, and generalizations of this modeling are discussed in Section 6.

The mechanics of the CEX are then straightforward: traders can swap any quantity  $y > 0$  of  $Y$  against  $yS_t^0$  of  $X$  while paying the fee  $\eta^0 y S_t^0$  (in units of  $X$ ) to third parties.

*DEX.* The DEX is implemented as constant product market maker (CPMM), akin to Uniswap v2.<sup>12</sup> The initial reserves  $(X_0, Y_0)$  of the two assets are seeded by a single representative liquidity provider (LP) who passively holds inventory of both assets and collects all trading fees that traders incur on the AMM.

Prices on the AMM are governed by the constant product invariant  $X_t Y_t = k$ , where  $(X_t, Y_t)$  are the reserves of the two assets at time  $t$ . The marginal price of  $Y$  is  $S_t^1 = X_t/Y_t$ , and the cost for trading a quantity  $\Delta$  of  $Y$  (positive for buy, negative for sell) is

$$P_t[\Delta] = \frac{X_t}{Y_t - \Delta}.$$

<sup>12</sup>Our simulation code is modular and can accommodate arbitrary AMM designs, for instance G3Ms.



After such a trade, the reserves update via

$$(2.2) \quad X_{t+\delta t} = X_t + P_t[\Delta] \cdot \Delta, \quad Y_{t+\delta t} = Y_t - \Delta,$$

and the new marginal price becomes

$$(2.3) \quad S_{t+\delta t}^1 = \frac{X_{t+\delta t}}{Y_{t+\delta t}} = \left( \frac{Y_t}{Y_t - \Delta} \right)^2 S_t^1.$$

A proportional fee  $\eta^1 > 0$  is charged on every DEX trade and paid directly to the LP (i.e., the amount  $\eta^1 P_t[\Delta]|\Delta|$  is paid in currency  $X$ ).<sup>13</sup> Since we assume that LPs do not mint or burn shares over time, the evolution of the reserves  $(X_t, Y_t)$  is entirely dictated by trader activity via (2.2).

*Traders.* In addition to the LP, two types of traders interact with the venues: fundamental traders and arbitrageurs. Fundamental traders have an exogenous trading motive whereas arbitrageurs only act when they can attain a round-trip profit from buying on one venue and immediately selling on the other.

Indeed, if the DEX offers a better sell price after fees than the CEX buy price after fees (or vice versa), arbitrageurs act to exploit the mispricing. For instance, if

$$S_t^0(1 + \eta^0) < S_t^1(1 - \eta^1)$$

it would be profitable to buy on the CEX and sell on the DEX. The size of the arbitrage trade is determined endogenously such as to maximize the profit, or equivalently, to align post-trade marginal prices (inclusive of fees). Explicitly, the arbitrageur's trade on the DEX is

$$(2.4) \quad \Delta_t^A = Y_t \left( 1 - \sqrt{\frac{S_t^1(1 - \eta^1)}{S_t^0(1 + \eta^0)}} \right) \wedge 0 + Y_t \left( 1 - \sqrt{\frac{S_t^1(1 + \eta^1)}{S_t^0(1 - \eta^0)}} \right) \vee 0.$$

On the other hand, fundamental traders have exogenous demand. They consist of fundamental buyers and sellers which must execute quantities  $\Delta_t^B > 0$  and  $\Delta_t^S < 0$ , respectively. While those quantities can be specified arbitrarily for each trading period of the simulation, we shall keep them constant over time for parsimony. Buyers and sellers act sequentially in randomized order: either buyers act first, or sellers. Their order flow is routed optimally between the venues, as though processed by a perfectly efficient aggregator (see Section 6 for a generalization). This means that traders send their marginal volume to the DEX if and only if the marginal price inclusive of fee is better than the price on the CEX inclusive of fee. Volume will be routed to the DEX until either the desired quantity is satisfied or the price on the DEX becomes aligned with the CEX (inclusive of fees). At that point, the remaining volume will be routed to the CEX as there is no price impact on the CEX. In formulas, buyers trade

$$(2.5) \quad \Delta_t^{B,DEX} = \left( \Delta_t^B \wedge Y_t \left( 1 - \sqrt{\frac{S_t^1(1 + \eta^1)}{S_t^0(1 + \eta^0)}} \right) \right) \vee 0$$

<sup>13</sup>In practice, two methods have been adopted for the collection of fees. Either fees are paid into a separate account, as in our model, or fees are deposited into the AMM pool. We have implemented both methods and found very similar results, thus use the method which leads to simpler formulas and has been favored in recent practice.

on the DEX and sellers trade

$$(2.6) \quad \Delta_t^{S,DEX} = \left( \Delta_t^S \vee Y_t \left( 1 - \sqrt{\frac{S_t^1(1-\eta^1)}{S_t^0(1-\eta^0)}} \right) \right) \wedge 0.$$

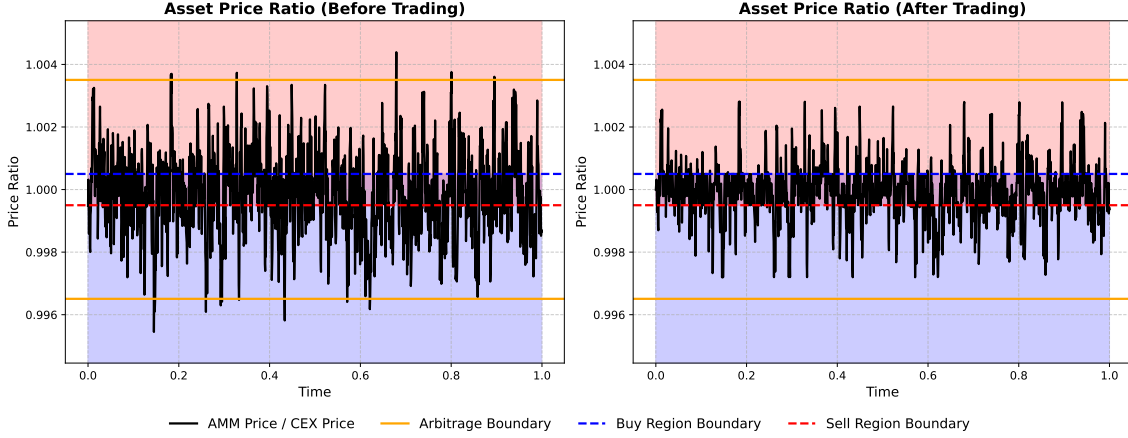


FIGURE 1. Sample trajectory of the asset price ratio  $R_t = S_t^1/S_t^0$  before and after trading on the DEX. Outside of the orange lines arbitrageurs act and reflect the price ratio. Above the red line the AMM captures fundamental sellers and the ratio is pushed down. Below the blue line the AMM captures fundamental buyers and the ratio is pushed up. The center band represents the region where the AMM captures both buy and sell flow. The figure shows the cumulative effect of arbitrageurs and fundamental traders.

We observe in Equations (2.4) to (2.6) that the decisions of all traders can be neatly expressed in terms of the *price ratio* process  $R_t = S_t^1/S_t^0$ . Comparing the above expressions, we see that buyers send marginal volume to the DEX if  $R_t < (1 + \eta^0)/(1 + \eta^1)$ , while seller volume arrives if  $R_t > (1 - \eta^0)/(1 - \eta^1)$ . Similarly, arbitrageurs trade if  $R_t < (1 - \eta^0)/(1 + \eta^1)$  or  $R_t > (1 + \eta^0)/(1 - \eta^1)$ . We call those thresholds the *buy region* boundary, *sell region* boundary, and *arbitrage region* boundaries, respectively. These regions will play a crucial role in our analysis of LP profitability; they are visualized alongside an illustrative evolution of  $R_t$  in Figure 1.

*LP PnL.* We evaluate LP performance through both unhedged and hedged profit-and-loss (PnL). Since we consider the CEX to be the primary venue of price formation, we mark holdings in  $Y$  to the CEX price (rather than the DEX price). The *unhedged (LP) PnL* is defined as the change in the marked-to-market value of the pool reserves plus the total of fees collected,

$$\text{Unhedged PnL} = X_T + Y_T \cdot S_T^0 - (X_0 + Y_0 \cdot S_0^0) + \text{Fees Accrued}.$$

When the price  $S_t^0$  is volatile, the unhedged PnL tends to be very noisy and primarily driven by the exposure to the price fluctuations of the  $Y$  holdings. Practitioners are more interested in the *hedged PnL* which isolates the effects of trading and fees by removing the price risk. Specifically, hedging takes place on the CEX; it proceeds by initializing a position of  $Y_0$  units of the risky asset and rebalancing each period to match the current  $Y_t$  reserve

level. We let  $H = (H_t)_{t \geq 0}$  denote the value of the hedging portfolio which is initialized at  $H_0 = X_0 + Y_0 S_0^0$  and updated in a self-financing fashion according to

$$H_{t+\delta t} = H_t + Y_t \cdot (S_{t+\delta t}^0 - S_t^0).$$

The cost of adjusting the hedge is computed using CEX prices and is frictionless in our baseline simulation.<sup>14</sup> The hedged LP PnL is therefore

$$\text{Hedged PnL} = \text{Unhedged PnL} - \sum_{i=1}^N Y_{(i-1)\delta t} \cdot (S_{i\delta t}^0 - S_{(i-1)\delta t}^0).$$

We see that when  $S^0$  is a martingale, the value of the hedging portfolio is given in terms of a martingale transform which is again a martingale. Throughout the paper, the *expected* PnL will be an important metric. Because of the martingale nature of the hedge, the expected value of the hedged and unhedged PnL are *identical*, hence either could be used. On a trajectory basis, the hedged PnL is significantly less noisy—as seen in the order of magnitude difference between the representative trajectories displayed in the lower panel of Figure 2.

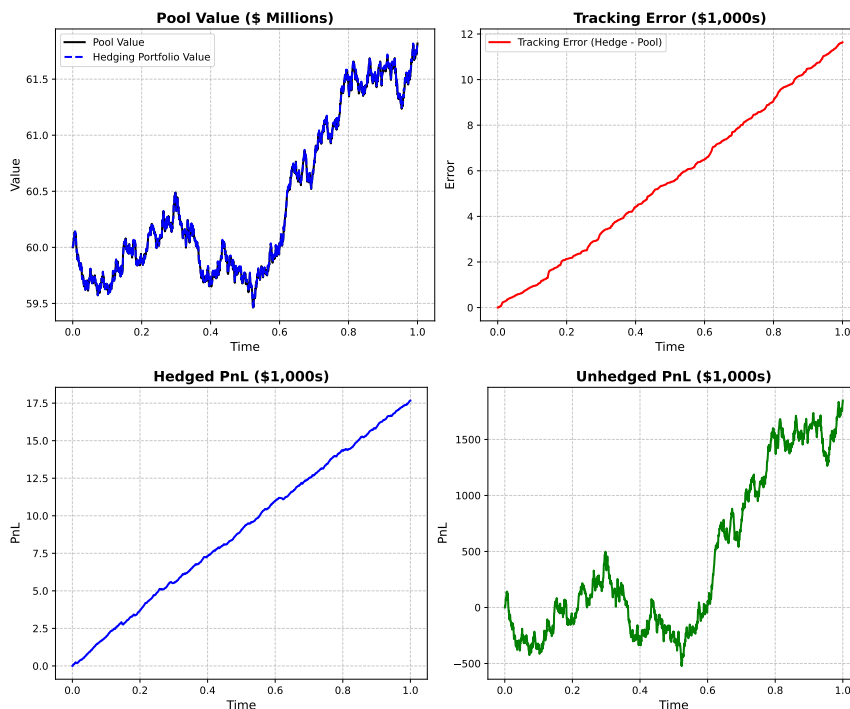


FIGURE 2. (Upper Left) Sample trajectory of the Pool Value  $X_t + Y_t S_t^0$  and hedging portfolio value  $H_t$ . (Upper Right) Corresponding evolution of the tracking error over time. (Bottom Left) Sample trajectory of Hedged PnL, to be compared with the Unhedged PnL (Bottom Right).

<sup>14</sup>For large LPs this simplifying assumption may be justified by internal netting. As an extension, our implementation also allows one to specify a separate, non-zero fee for hedge trades; this is discussed in Section 6.

It is useful to group the pool value and hedge value into a single term, the *tracking error*,

$$\text{Tracking Error} = H_t - X_t - Y_t \cdot S_t^0,$$

so that we may write

$$\text{Hedged PnL} = \text{Fees Accrued} - \text{Tracking Error}.$$

The tracking error is exactly the loss-versus-rebalancing (LVR) of [31] except that we mark asset values to the CEX price instead of the DEX. It can be thought of as reflecting LP losses that are attributable to the adverse selection on the DEX brought on by stale prices. A visualization of the tracking error is given in the upper right panel of Figure 2.

*Simulation Steps.* We adopt a turn-based simulation in which each period of length  $\delta t$  is subdivided into four further steps:

1. The CEX price is incremented.
2. Arbitrageurs compare the new CEX price with the DEX price and, if applicable, execute a roundtrip trade of size (2.4). This trade changes the marginal DEX price according to (2.3), removing the arbitrage opportunity.
3. An independent coin-flip decides whether fundamental buyers or sellers move first. In the former case, buyers trade quantity (2.5) on the DEX whose marginal price adjusts according to (2.3). Next, sellers trade quantity (2.6) on the DEX, again changing its price. In the latter case, the order is reversed.
4. The LP updates their hedging portfolio on the CEX.

The simulation loops over those steps; Appendix A provides pseudocode summarizing the implementation. Some models in the literature use noise traders whose actions can lead to arbitrage opportunities, hence those models include a second intervention of arbitrageurs exploiting those. In the present baseline model, the actions of fundamental traders in Step 3 never create arbitrage opportunities, hence it would be futile to include another arbitrageur trade.

### 3. DETERMINANTS OF LP PROFITABILITY

In this section, we examine how LP profitability is influenced by fundamental demand, market volatility, and fee levels. To that end, we investigate the comparative statics of the simulation model described in the preceding section.

Our baseline considers a one-day trading horizon with a one-minute time resolution, corresponding to  $T = 1$  and  $N = 1440$ . The AMM is initialized with \$30,000,000 in numéraire reserves ( $X$ ) and 10,000 units of the risky asset ( $Y$ ), implying an initial price of  $S_0^1 = \$3,000$  and a total pool value of \$60,000,000. Prices on the CEX are set to the same initial value,  $S_0^0 = \$3,000$ , and evolve according to (2.1) with volatility  $\sigma = 0.04$ . The default CEX fee is  $\eta^0 = 20$  basis points (bps). Fundamental buy and sell demand arrives at a rate of 5,000 units of  $Y$  per day, uniformly distributed across time (i.e.,  $\Delta_t^B = -\Delta_t^S = 5,000 \cdot \delta t$  per minute), which corresponds to a total unsigned daily demand of 10,000 units or 100% of the pool’s initial inventory. This configuration serves as a reference point for our analysis. A detailed discussion of the plausibility of these benchmark values, including an empirical calibration to real market data, is provided in Section 5.

We begin by motivating our use of *expected* PnL as a performance metric for LPs. Figure 3 shows the distribution of terminal hedged PnL across different AMM fee levels. While the PnL variance changes only modestly with the fee, the expected PnL is much more sensitive.

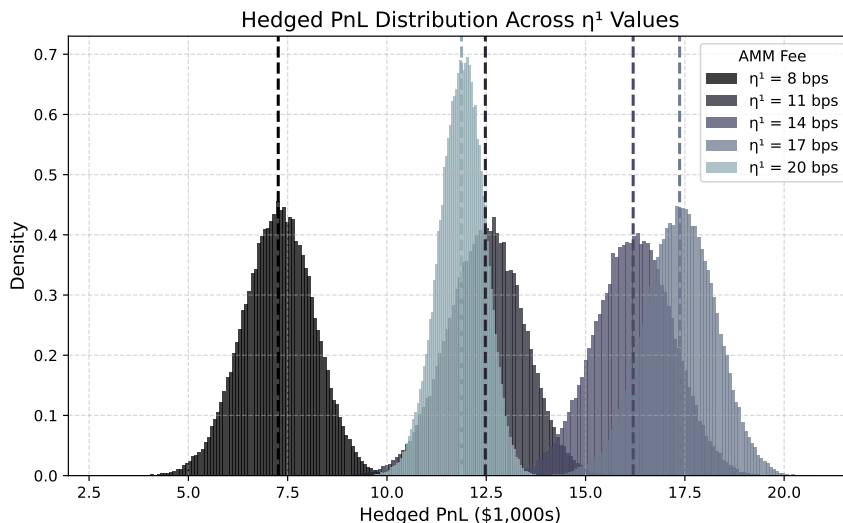


FIGURE 3. Histograms of terminal hedged PnL across 100,000 simulations, colored by AMM fee level. Dashed lines mark the distribution means.

Moreover, some fee levels consistently outperform others, and PnL is *not* monotonic in the fee level, highlighting its central role in determining LP returns.

Before delving into the details, we observe two basic features of LP profitability. Figure 4 plots average PnL across varying levels of fundamental demand and volatility, holding the AMM fee fixed at  $\eta^1 = 15$  bps.

Two broad patterns emerge: expected PnL declines with volatility and increases with the size of fundamental demand. The detailed analysis in this section will show how greater price dispersion increases the likelihood of stale execution and adverse selection, lowering PnL. On the other hand, when more flow interacts with the AMM, the LP earns more fee revenue. More importantly, we will see that this additional fundamental flow tends to trade at prices that are less stale, an effect not seen in previous models with only (uninformed) noise traders.

**3.1. The Price Ratio.** The ratio between AMM and CEX price is a key quantity to understand why trades generate gains or losses for the LP. Following the concept of toxic vs. benign flow in classical finance, it is tempting to think of arbitrageur trades as inherently “bad” for the LP and fundamental trades as “good.” However, this dichotomy is misleading. The next part of our analysis builds on a key insight: whether a trade benefits or harms the LP does not depend on the identity or intent of the trader, but rather on the *price ratio* at which the trade occurs.

To build intuition, we characterize the conditions under which a marginal (infinitesimally small) trade on the DEX yields a profit for the LP, accounting for hedging activity on the CEX. Suppose a trader executes a small buy order of size  $\Delta > 0$  units of the risky asset  $Y$ . The LP gives up  $\Delta$  units of  $Y$ , receives approximately  $\Delta \cdot S_t^1$  units of the numéraire asset  $X$  at the current AMM price, and collects an additional fee of  $\eta^1 \cdot \Delta \cdot S_t^1$ . To maintain a neutral inventory, the LP rebalances by purchasing  $\Delta$  units of  $Y$  on the CEX at price  $S_t^0$ , incurring a cost of  $\Delta \cdot S_t^0$ . The marginal change in the LP’s hedged PnL (expressed in units

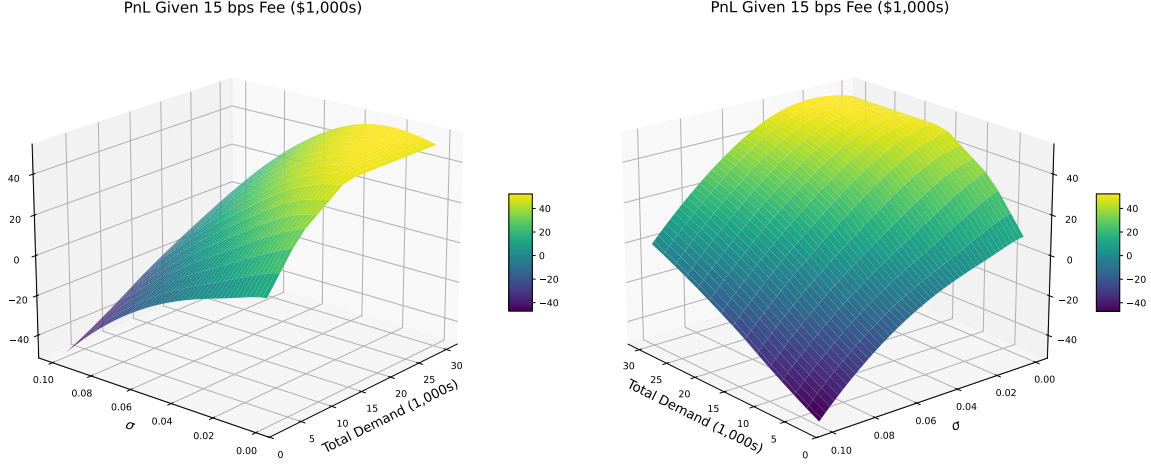


FIGURE 4. Expected PnL as a function of fundamental demand and volatility under the baseline AMM fee of 15 bps. The left and right figures show two different orientations of the same surface.

TABLE 1. Trading and Profitability Thresholds

	Trade Condition	Profit Condition
<b>Fundamental Buyers</b>	$R_t \leq \frac{1 + \eta^0}{1 + \eta^1}$	$R_t \geq \frac{1}{1 + \eta^1}$
<b>Fundamental Sellers</b>	$R_t \geq \frac{1 - \eta^0}{1 - \eta^1}$	$R_t \leq \frac{1}{1 - \eta^1}$
<b>Arbitrage Buyers</b>	$R_t \leq \frac{1 - \eta^0}{1 + \eta^1}$	N/A
<b>Arbitrage Sellers</b>	$R_t \geq \frac{1 + \eta^0}{1 - \eta^1}$	N/A

of  $X$ ) is therefore

$$\text{Change in Hedged PnL} \approx \Delta \cdot [(1 + \eta^1)S_t^1 - S_t^0] = \Delta \cdot S_t^0 [(1 + \eta^1)R_t - 1].$$

Similarly, for a small sell trade  $\Delta < 0$ , the LP receives  $|\Delta|$  units of  $Y$ , pays  $|\Delta| \cdot S_t^1$  in  $X$ , and hedges by selling  $|\Delta|$  units of  $Y$  on the CEX at price  $S_t^0$ , yielding a revenue of  $|\Delta| \cdot S_t^0$ . The resulting impact on the hedged PnL is

$$\text{Change in Hedged PnL} \approx \Delta \cdot [(1 - \eta^1)S_t^1 - S_t^0] = \Delta \cdot S_t^0 [(1 - \eta^1)R_t - 1].$$

Evidently, for a buy trade ( $\Delta > 0$ ), the LP earns a profit on a marginal trade if and only if  $R_t > 1/(1 + \eta^1)$ . For a sell trade ( $\Delta < 0$ ), the LP earns a profit on a marginal trade if and only if  $R_t < 1/(1 - \eta^1)$ . We combine these thresholds with those of the preceding section in Table 1, and illustrate their sensitivity to the choice of the AMM fee  $\eta^1$  in Figure 5.

We see that the LP benefits from trades that occur when the AMM price does not deviate too far from the CEX reference. In particular, *both* buy and sell trades are profitable for

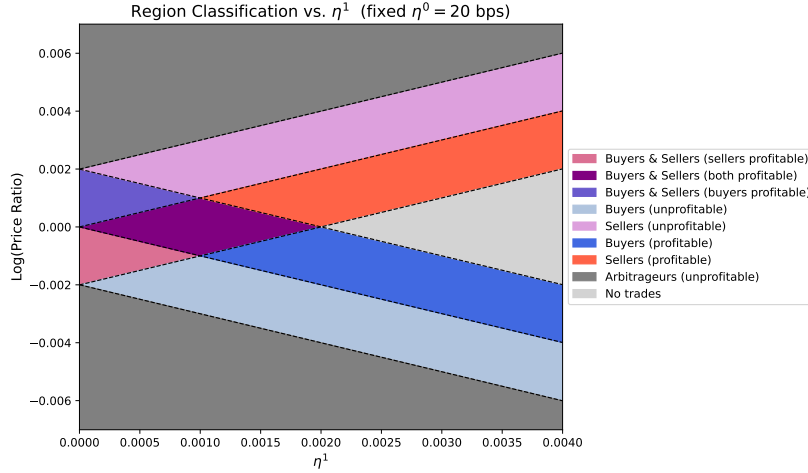


FIGURE 5. Illustration of how the critical regions from Table 1 change with the AMM fee  $\eta^1$ , shown in terms of the log price ratio.

the LP when the price ratio lies within the interval

$$\left[ \frac{1}{1 + \eta^1}, \frac{1}{1 - \eta^1} \right].$$

We refer to this as the *profit region*: any marginal trade occurring within this band yields a net gain for the hedged LP, regardless of trade direction. Outside this region, one side of the market results in a loss for the LP, even if the flow originates from fundamental traders.

A related concept is the *buy-sell region*, defined (when  $\eta^1 \leq \eta^0$ ) by

$$\left[ \frac{1 - \eta^0}{1 - \eta^1}, \frac{1 + \eta^0}{1 - \eta^1} \right].$$

This is the range of price ratios in which both fundamental buyers and sellers prefer trading on the AMM over the CEX, allowing the LP to capture two-sided flow. When  $\eta^1 > \eta^0$ , this region becomes empty and the DEX is never simultaneously optimal for both sides of the market.

Crucially, the profit and buy-sell regions respond differently to the AMM fee  $\eta^1$ , and there is no consistent inclusion relationship between them. As  $\eta^1$  increases, the profit region expands but the buy-sell region shrinks. Figure 5 illustrates this interaction. When  $\eta^1$  is small, it is possible for the buy and sell thresholds to lie outside the profit region, meaning the LP captures two-sided flow even when some trades are marginally unprofitable. By contrast, as  $\eta^1 \uparrow \eta^0$ , the profit region will fully contain the buy-sell boundaries.

When the price ratio leaves the broader *no-arbitrage region*

$$\left[ \frac{1 - \eta^0}{1 + \eta^1}, \frac{1 + \eta^0}{1 + \eta^1} \right],$$

arbitrageurs intervene to realign prices across venues. The no-arbitrage region always contains the profit region, since  $\eta^0 \geq 0$ , and arbitrage trades—by construction—are *always unprofitable* for the LP. Figure 5 demonstrates that as  $\eta^1$  increases, the arbitrage thresholds are pushed outwards. While this reduces the frequency of loss-making arbitrage trades, from the LP's perspective this should be balanced by the effects on the other regions.

Our model can be compared to the one of Glosten and Milgrom [22]. There, market makers defensively widen spreads because they cannot distinguish benign flow from informed flow that predicts future price movements. Here, fees play an analogous role, as the AMM fee cannot depend on the current CEX price or the trader motive.

**3.2. Distribution of the Price Ratio.** The preceding classification of regions provides a static view of trade incentives and profitability but offers no insight into how often the AMM/CEX price ratio falls within each region. Next, we study the distribution of the price ratio, which determines the occupation times of the profit, buy-sell, and arbitrage bands, and hence offers first insights into the LP PnL.

**3.2.1. Sensitivity to Fees.** The first row of Figure 6 shows histograms of the log price ratio,  $\log(R_t) = \log(S_t^1/S_t^0)$ , sampled immediately *before* trade execution (i.e., between Steps 1 and 2 as listed at the end of Section 2), across various AMM fee levels ranging from 5 to 25 basis points. The second row of Figure 6 illustrates the closely related influence of the CEX fee on the price ratio distribution. These distributions are computed using data from 100,000 simulation runs, aggregated over all time steps. When one parameter is varied, the others are set to the baseline values introduced at the beginning of this section. Simulation statistics like expected profit and volume captured are reported in Appendix B.

At low AMM fee levels relative to the CEX (e.g.,  $\eta^1 = 5$  bps and  $\eta^0 = 20$  bps, or  $\eta^1 = 15$  bps and  $\eta^0 = 60$  bps), the AMM offers competitive execution and captures a large share of trading volume. The buy-sell region is wide, and the resulting bidirectional fundamental flow flattens the central portion of the distribution. Indeed, when buy and sell trades compensate one another, the log ratio process locally resembles a Brownian motion without drift. The flat part of the distribution (see the second row and last column of Figure 6 for a pronounced example) can be compared to the stationary distribution of Brownian motion reflected in a strip, which is a uniform distribution. Overall, this regime produces a broad and diffuse shape. While a large fraction of the transactions originates from fundamental traders, many of the trades occur at price ratios outside the LP’s profit region, leading to poor PnL despite high turnover.

As the AMM fee increases, the widening of the profit region and the decline in the AMM’s competitiveness restrict participation to trades that remain viable despite the higher cost. This leads to a contraction of the price ratio distribution around its center due to the price impact of asymmetric fundamental flow: when only one side of the market interacts with the AMM, trade flow pushes prices directionally. At high (relative) fees (e.g.,  $\eta^1 \geq \eta^0 = 20$  bps), only unilateral flow is captured and this effect becomes most pronounced. In fact, when  $\eta^1 > \eta^0$  the order of the buy and sell boundaries switches so that they enclose a region where the AMM receives *no* order flow. At the same time, a widening of the no-arbitrage region leads to slightly longer tails of the distribution at large values of  $\eta^1$ . The overall effect of increasing  $\eta^1$  is thus a transition from high-turnover, low-margin activity with relatively diffuse pricing to high-margin, selective trading centered near the CEX price.

While both the AMM and CEX fees expand the arbitrage region by pushing the arbitrage thresholds outward, an important distinction arises in their impact on the buy-sell region. Specifically, increasing the AMM fee shrinks this region, while increasing the CEX fee expands it by making AMM execution comparatively more favorable for fundamental traders. The net effect is a broader, flatter ratio distribution as  $\eta^0$  increases. Notably, although the CEX fee modifies the attractiveness of AMM execution, it leaves the boundaries of the LP’s profit region unaffected.



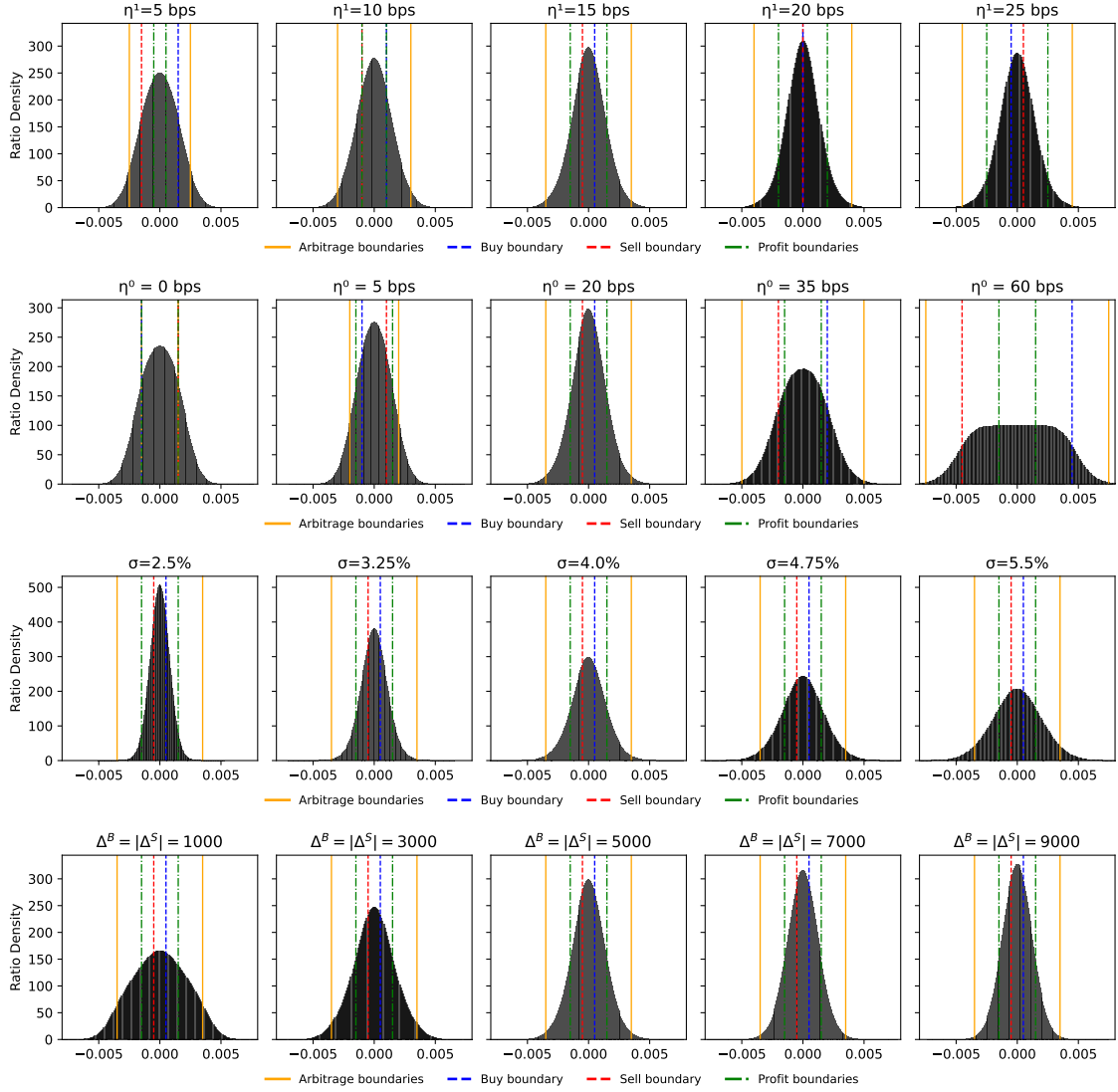


FIGURE 6. Distributions of the log price ratio  $\log(R_t) = \log(S_t^1/S_t^0)$  sampled immediately before trade execution. The center panel of each row corresponds to the common benchmark setting:  $\eta^1 = 15$  bps,  $\eta^0 = 20$  bps,  $\sigma = 4\%$ , and  $\Delta^B = |\Delta^S| = 5,000$ . Each row illustrates how the shape of this distribution varies with (top) the AMM fee  $\eta^1$ , (second) the CEX fee  $\eta^0$ , (third) market volatility  $\sigma$ , and (bottom) fundamental demand. Distributions are aggregated over 100,000 simulation paths. All other parameters follow the baseline specification in Section 3. Statistics for each configuration are reported in Appendix B.

3.2.2. *Sensitivity to Volatility.* The third row of Figure 6 depicts how the log price ratio distribution changes with market volatility  $\sigma$  when the AMM fee  $\eta^1$  is fixed at 15 bps. At low volatility (e.g.,  $\sigma = 2.5\%$ ), the distribution is sharply concentrated near zero. In this regime, the reference price evolves gradually, and fundamental order flow acts as a

stabilizing force: when the price ratio escapes the buy-sell region, the impact from one-sided trading is often enough to push the ratio back in and keep prices closely aligned with the CEX, without any action from arbitrageurs. As a result, the AMM captures a large share of fundamental flow, with much of it arriving in the profit region for this fee level (see Appendix B for the numerical values).

As volatility increases, the distribution of  $\log(R_t)$  becomes increasingly dispersed. At high values of  $\sigma$ , fundamental demand is unable to adjust the AMM price by enough to track the large swings in the reference price. This leads to more frequent and severe price misalignments. A large number of trades occur outside of the profit region and at the highest value illustrated,  $\sigma = 5.5\%$ , a nontrivial fraction of the trades occur outside of the arbitrage boundaries, implying that they are arbitrageur trades. This widening of the price ratio distribution at high volatility levels contributes to the deterioration in LP profitability observed above.

**3.2.3. Sensitivity to Demand.** The last row of Figure 6 illustrates how the distribution of the log price ratio evolves with increasing levels of fundamental demand when  $\eta^1 = 15$  bps. At low levels of demand, the ratio distribution has a broad and bulbous shape, and a large fraction of the trading volume arrives while the price ratio is outside of the profit region. As demand increases, we observe a notable increase in the concentration of the distribution about zero.

This behavior can be attributed to the stronger directional pressure exerted by fundamental order flow. When demand is weak, price adjustments are sluggish and the AMM quotes often lag behind the CEX value, which exposes the pool to adverse selection. As demand increases, the consistent push from one-sided flow outside of the buy-sell region creates a stabilizing drift that keeps AMM prices more tightly aligned with the CEX. The result is twofold: not only does higher demand increase traded volume and hence the fee revenue, but it also enhances the quality of execution from the LP’s perspective. (Of course, there is a limit to this effect: even if fundamental demand were infinite, the finite liquidity in the pool ensures that price impact would grow until traders are incentivized to transact on the CEX.)

**3.3. Trading Volume and Market Demand.** Understanding where the price ratio spends time is only part of the picture—LP profitability hinges on how much volume is transacted in each region and the fees earned per trade. Fundamental order flow is directed to the AMM when it offers better execution than the CEX for buy or sell orders. The competitiveness of the AMM’s pricing, and hence the volume it captures, is shaped by the AMM fee  $\eta^1$  and market volatility  $\sigma$ . Because fundamental traders are the *only* source of profitable volume (see Section 3.1), it is critical to understand this relationship.

Figure 7 shows the expected volume of fundamental trades executed by the AMM and the associated fee revenue over the simulation horizon. Since prices remain relatively stable over the course of a day, fee revenue is roughly proportional to the product of captured volume and the fee level  $\eta^1$ . The most striking insight of Figure 7 is that, except at very high volatility, volume and revenue strongly depend on the relationship between AMM and CEX fee. At low volatility, even modestly undercutting the CEX fee enables the AMM to capture almost all of the fundamental flow; a more detailed discussion of this undercutting will follow in Section 4 in the context of optimizing the AMM fee. While this effect is reduced as volatility increases, it remains important in a range of volatilities. As volatility increases, AMM prices become stale more quickly, reducing their competitiveness.

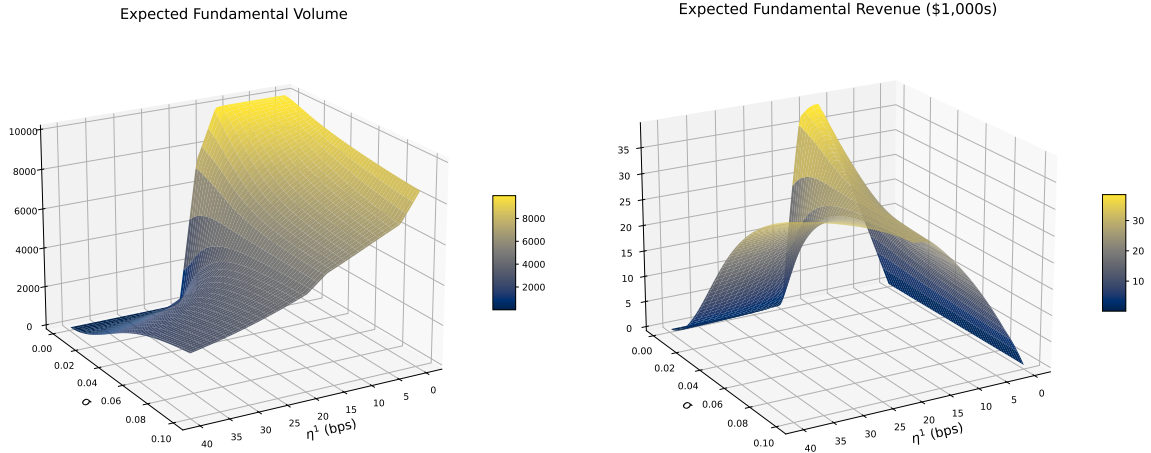


FIGURE 7. (Left) Expected fundamental trader volume received by the AMM as a function of  $\eta^1$  and  $\sigma$ . (Right) Corresponding fee revenue. Lower volatility favors high capture rates, while revenue reflects the interaction of volume and fee level.

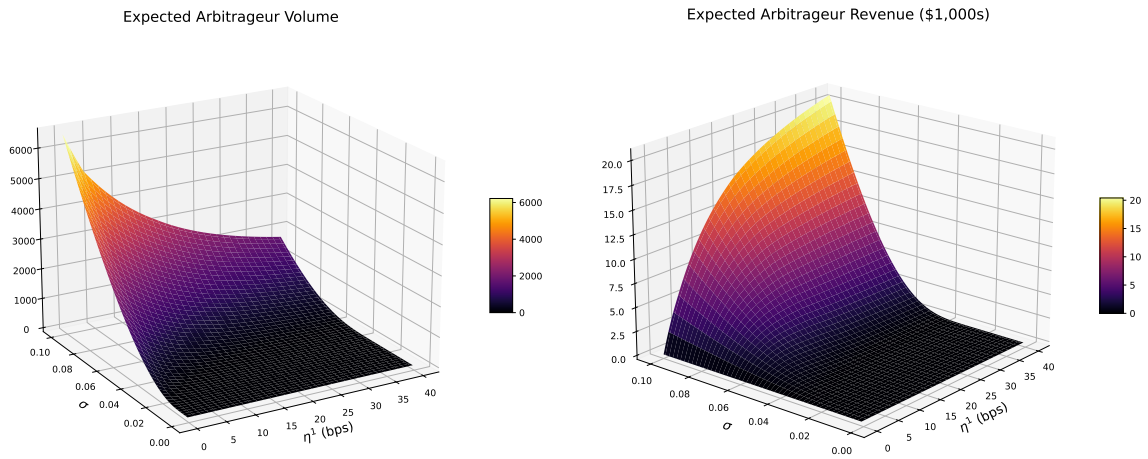


FIGURE 8. (Left) Average arbitrageur volume received by the AMM across combinations of AMM fee  $\eta^1$  and volatility  $\sigma$ . Higher volatility increases arbitrage activity, while higher fees reduce it. (Right) Associated fee revenue earned from these trades.

Maintaining volume under these conditions requires lowering fees, but this comes at the cost of reduced revenue per trade. The result is a fundamental economic trade-off: greater competitiveness erodes margins, and this tension intensifies in more volatile markets.

On the other hand, the relationship between arbitrage activity, AMM fee, and volatility is relatively straightforward. Higher volatility increases price discrepancies between the AMM and the CEX and hence the arbitrageur volume, as shown in the left panel of Figure 8. By contrast, higher AMM fees reduce arbitrage incentives and thus lower arbitrage flow. The

right panel reports the associated fee revenue from these trades. Although this revenue can be considerable in high-volatility and high-fee settings, it is not sufficient to offset the losses from adverse selection (as shown analytically in Section 3.1).

#### 4. OPTIMAL FEES AND LP PERFORMANCE

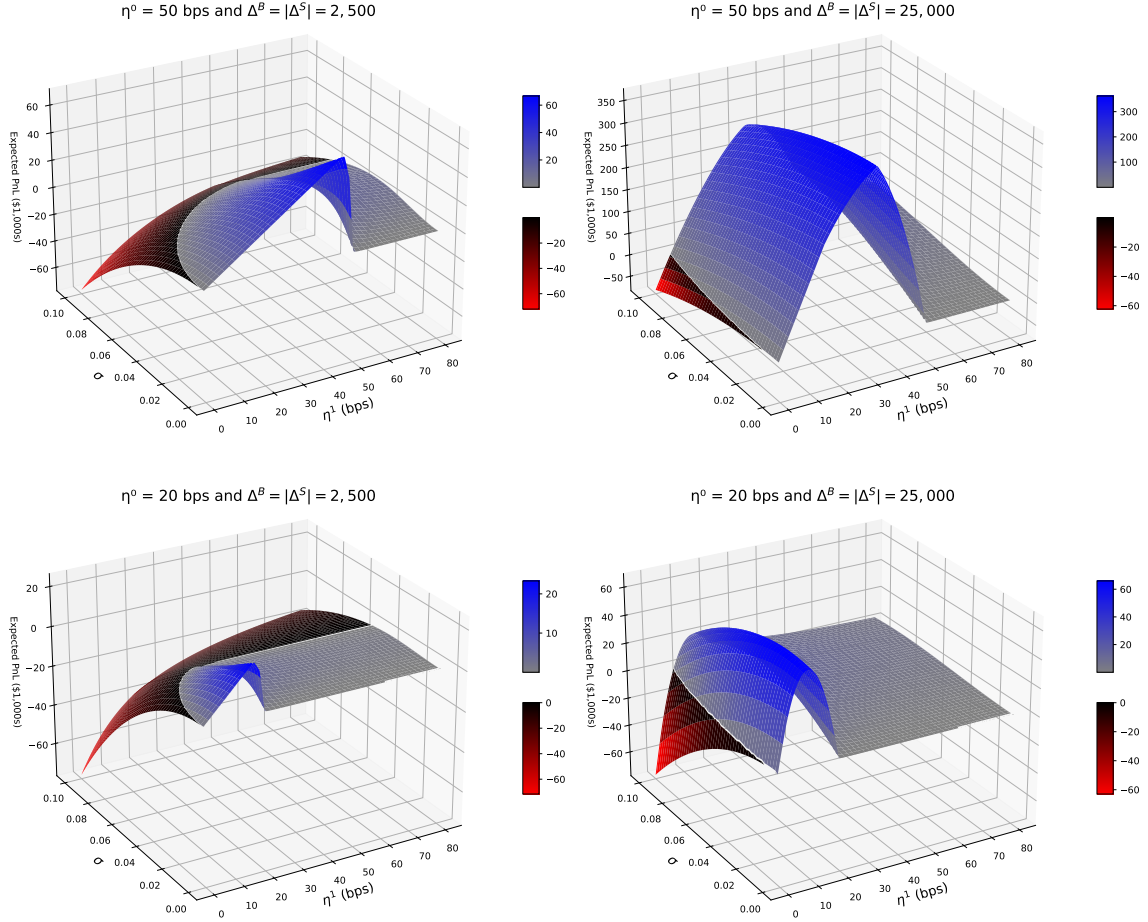


FIGURE 9. Expected PnL surface as a function of the AMM fee  $\eta^1$  and market volatility  $\sigma$ , shown under two different assumptions about fundamental demand and CEX fee  $\eta^0$ . The bottom row corresponds to the baseline fee of  $\eta^0 = 20$  bps while the top row uses  $\eta^0 = 50$  bps. The left column illustrates a demand of  $\Delta^B = |\Delta^S| = 2,500$ , below our baseline, while the right column increases demand to the (very high) level of  $\Delta^B = |\Delta^S| = 25,000$ . The expected PnL for our baseline of  $\Delta^B = |\Delta^S| = 5,000$  is represented in the right panel of Figure 10 below.

The preceding discussion highlighted that the AMM fee  $\eta^1$  governs a trade-off: higher fees increase per-trade revenues for the LP and defend against adverse selection; at the same time, they reduce the AMM's competitiveness, lowering the volume of fundamental

order flow it attracts and increasing price stickiness. In this section, we distill these interactions and determine the AMM fee level that maximizes LP profitability for given market conditions.

Figure 9 plots the expected PnL surface as a function of  $\eta^1$  and volatility  $\sigma$ , for varying levels of fundamental demand and different CEX fee benchmarks  $\eta^0$ . A consistent pattern emerges: for a broad range of volatilities  $\sigma$ , the optimal fee is strictly less than the CEX fee, with the PnL surface exhibiting an interior maximum below  $\eta^0$ . The maximum is particularly pronounced for moderate volatility. As the CEX fee increases, the peak of the surface shifts by a similar amount. In brief, the optimal fee for the AMM is to *undercut* the CEX fee.

At this point it may be important to recall that our CEX fee  $\eta^0$  is a reduced-form representation of the effective execution cost faced by market participants, not merely the nominal fee posted by the exchange. Moreover, in practice, this cost (as well as the posted fee) varies substantially across traders due to tiered fee schedules, volume-based discounts and rebates, and optimal execution algorithms employed by sophisticated traders. Our parsimonious model absorbs these nuances into a single parameter  $\eta^0$ , representing an average or effective benchmark. Consequently, the aforementioned undercutting does not mean that the optimal AMM fee is lower, e.g., than a posted headline rate such as Binance’s taker fee, but rather that it should remain competitive with the distribution of effective CEX trading costs.<sup>15</sup> A calibration to real-world data is provided in Section 5, and generalizations of the fee structure are also discussed in Section 6.3.

Returning to Figure 9, we observe that increased volatility depresses PnL across all fee levels, while increased demand raises it. At high levels of volatility, the interior maximum disappears and expected PnL turns *negative* across all plausible fee values, indicating that the LP would prefer an infinite AMM fee to prevent trading.

We also observe that greater demand smooths the relationship between PnL and optimal AMM fee, consistent with the notion that an abundance of available order flow reduces the sensitivity of performance to fee design. Of course, there is a limit to this effect. At the extremes of demand, the liquidity in the pool is insufficient to absorb any marginal flow. Likewise, at very high fee levels and low volatility, it is almost never optimal for traders to engage with the pool regardless of aggregate demand.

The important Figure 10 extracts from the PnL surface the functional relationship between the optimal fee and market volatility  $\sigma$  for several levels of fundamental demand. Overall, we observe a fairly complex behavior in the left panel—but note that the figure shows a very wide parameter range. Next, we discuss this behavior, going from low to high demand, or from the top-left to bottom-right curve. While we explain in detail how all the shapes—including extreme regimes—are implied by the model, we emphasize that the most important regime for practical purposes is likely closer to the benchmark regime discussed in Sections 4.3 and 4.4 below.

**4.1. Low Demand.** For low to moderate levels of demand (darkest curves in the left panel of Figure 10), the optimal fee exhibits a U-shape in  $\sigma$ , which we explain first.

<sup>15</sup>For very large demand, a proportional fee may not be a good proxy for price impact costs on the CEX. Additional price impact would likely increase the optimal AMM fee, as the AMM competes with the overall slippage on the CEX. We remark that adding nonlinear price impact on the CEX would substantially complicate the order routing discussed in Section 2.

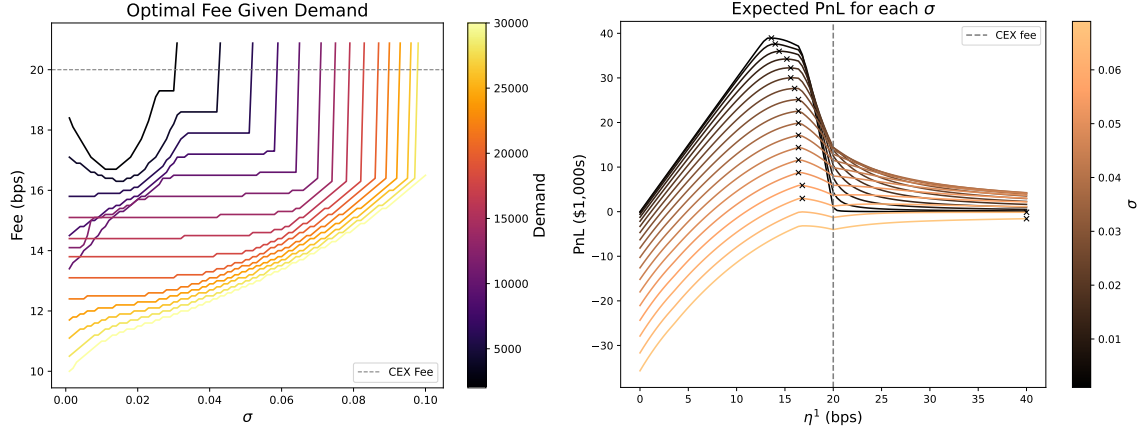


FIGURE 10. (Left) Optimal AMM fee as function of volatility, for several levels of total fundamental demand  $\Delta^B + |\Delta^S|$ . (Right) Expected PnL as a function of the AMM fee (for the baseline total demand of 10,000) with the numerically optimal fee marked by  $\times$ , for several levels of volatility. Where  $\times$  is at 40 bps, the PnL is always negative and the true optimum is  $\eta^1 = \infty$ .

When there is no volatility (i.e.,  $\sigma = 0$ ), the AMM can capture *all* of the fundamental demand by undercutting the CEX by just enough to remain the preferred venue after accounting for price impact. While there is still a nonlinear relationship between LP profit and fee levels due to the influence of  $\eta^1$  on demand, this is a good proxy for what happens when demand is low. Indeed, if  $\Delta^B = |\Delta^S| \approx 0$  and  $\sigma = 0$  then the buyers have next to no price impact and (since  $S_t^1 \approx S_t^0 \equiv S_0^0 = S_0^1$ )

$$\text{Fee Revenue} \approx \eta^1 (\Delta^B + |\Delta^S|) S_0^1 \mathbb{1}_{\{\eta^1 < \eta^0\}}.$$

This is clearly maximized by taking  $\eta^1$  arbitrarily close (but not equal) to  $\eta^0$ .

For these lower demand levels, the gap between the CEX fee and the left endpoint of the curves in Figure 10 (left panel) is approximately such that the AMM remains the preferred venue even after most of the fundamental buyers (or sellers) pushed its price in one direction. As a result, the gap initially increases with fundamental demand. Since the external price is constant, there is no possibility of arbitrage in this environment. This story persists in very low-volatility environments. Indeed, since prices are relatively stable, the AMM can undercut the CEX by a modest amount and still attract the lion's share of the fundamental volume.

As volatility starts to increase, the fluctuations in the reference price become more of a concern as AMM quotes become stale more quickly. Nonetheless, the dominant theme for low volatility is volume capture. Remaining competitive in this environment requires a deeper fee discount, leading to a decline in the optimal fee (the decreasing part of the U-shape). At intermediate levels of volatility, the directional pressure from fundamental flow is no longer sufficient to keep prices aligned. In this regime, the optimal fee flattens out, reflecting a delicate balance between capturing order flow and earning adequate revenue per trade.

Beyond a critical volatility threshold, adverse selection begins to dominate the LP's decisions. The optimal fee starts to rise—gradually at first, and then more quickly—as

the LP shifts focus from volume to per-trade PnL and aims to avoid severely unprofitable executions. Eventually, the optimal fee reaches a plateau below the CEX fee. This plateau represents the stability of the argmax also seen in the right panel of Figure 10 (shown there for higher demand). It remains near this level until a tipping point is reached: when volatility becomes too severe, expected PnL is negative for all fee levels and essentially increasing in  $\eta^1$ . At this stage, the optimal fee jumps to  $+\infty$ , signaling that the LP would prefer to shut down AMM activity.

**4.2. Moderate to High Demand.** As fundamental demand increases, the dependence of the optimal fee on volatility  $\sigma$  becomes monotonically increasing. We also observe that the optimal fee for  $\sigma = 0$  decreases, toward approximately  $\eta^0/2 = 10$  bps for very large demand.<sup>16</sup>

The limit of  $\eta^0/2 = 10$  bps can be understood analytically as follows. In the regime of high demand, DEX liquidity remains finite, so the LP can only absorb a limited amount of volume per time step. With abundant demand, buyers push the price ratio to the buy boundary, and sellers push it to the sell boundary. Over time, the system oscillates between these two points. By assuming we initialize the system at one of these boundaries and randomizing the arrival of buyers and sellers, the AMM captures both sides of the market 50% of the time, and one-sided trades otherwise. In expectation, this results in fee revenue equivalent to 75% of a round-trip price movement from the buy boundary to the sell boundary and back. Since the CEX price remains constant for  $\sigma = 0$ , both trade sizes and LP proceeds are deterministic and can be computed explicitly. By expanding for small  $\eta^0, \eta^1$ , we obtain the following leading-order approximation for the expected revenues (see Appendix C for details)

$$\frac{1}{N} \mathbb{E}[\text{Fee Revenue}] \approx \frac{3}{4} X_0 (2\eta^1 \eta^0 - 2(\eta^1)^2).$$

Maximizing this expression with respect to  $\eta^1$  yields the approximate optimal fee  $\eta^{1,*} \approx \eta^0/2$  which is consistent with the behavior observed in Figure 10.

At this fee level, the LP’s profit boundaries and the buy-sell boundaries are nearly identical (see Table 1). We conclude that, in this regime, the LP’s objective shifts from maximizing order flow capture to optimizing fee revenue per unit of volume. This perspective also clarifies why the optimal fee becomes strictly increasing in volatility  $\sigma$  as demand grows. In low-demand settings, higher volatility reduces the AMM’s competitiveness by making prices stale, necessitating lower fees to maintain flow capture. However, in high-demand environments—where price ratios naturally hover near the profit boundaries due to high levels of fundamental trading—volatility introduces the risk of prices drifting into unprofitable regions. To mitigate this, the LP increases fees, providing a buffer that preserves favorable execution conditions.

That said, even with elevated demand, extreme volatility renders price swings so severe that continued AMM operation becomes unprofitable, motivating the LP to once more exit the market by setting prohibitively high fees, explaining the vertical part of the curves.

**4.3. Benchmark Performance.** The right panel of Figure 10 depicts the expected PnL as a function of the AMM fee across a range of  $\sigma$  when demand is fixed at the baseline

<sup>16</sup>For low volatility regimes, the monotonicity of the optimal fee in demand breaks down at an intermediate point. This is elucidated in Figure 23 of Appendix C.1, which illustrates that a shift in the expected PnL curve’s maximum is responsible for this behavior.

of  $\Delta^B = |\Delta^S| = 5,000$  (i.e., 10,000 units in total). The maxima corresponding to the left panel of the figure are indicated by  $\times$  markers. This demand falls squarely between the two extremes discussed above. At this level, we no longer observe the decreasing part of the U-shape that was prevalent at the lowest total demands of 2,000-4,000 units. At the same time, we do not undercut the CEX as much as in the highest levels of 20,000-30,000 units. In this intermediate regime, we see that when volatility is low, PnL is sharply peaked, and too high of a fee can meaningfully impair performance. As volatility increases, the curvature around the PnL maximum decreases, indicating reduced sensitivity to fee choice near the optimum. Nonetheless, in the highest volatility regimes where PnL is always negative, undercutting the CEX is extremely undesirable and any fee that allows for a meaningful trading volume can result in significant losses.

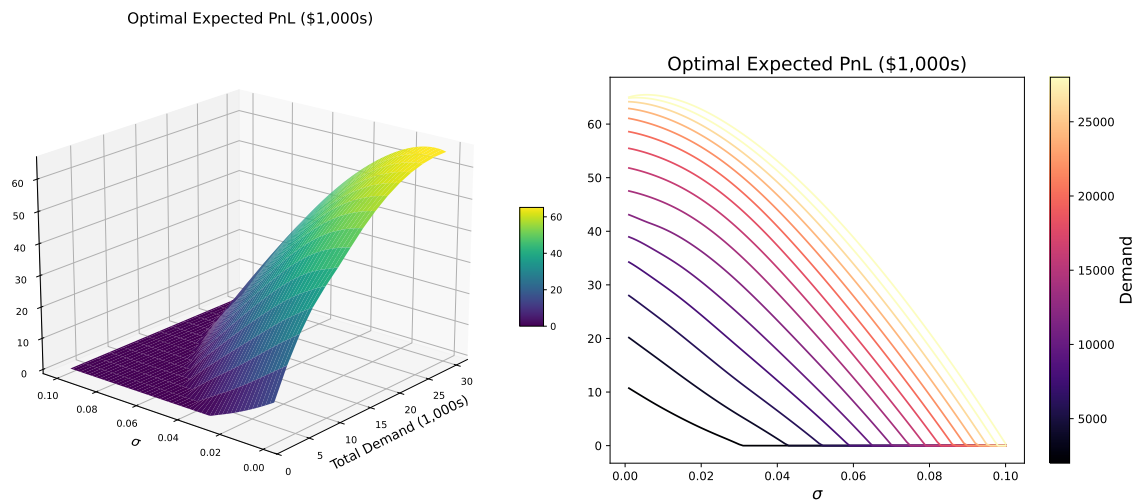


FIGURE 11. (Left) Expected PnL surface under optimal fees from Figure 10, shown as a function of volatility  $\sigma$  and total fundamental demand  $\Delta^B + |\Delta^S|$ . (Right) Cross-section of the same surface as a function of  $\sigma$ , with total demand levels indicated by the color gradient.

**4.4. Takeaways.** Notably, for a broad range of intermediate volatility levels, a suitably chosen constant fee performs reasonably well. Whereas, for very high volatility (relative to demand) it is optimal for the LP to quote a prohibitively high fee, effectively shutting down trading. This behavior aligns with established practice in traditional financial markets: during market shocks, it is often prudent to widen spreads substantially—or even halt trading altogether—to mitigate risk.

Figure 11 shows the expected PnL achieved under the optimal fee for each combination of fundamental demand and volatility. Consistent with our original findings in Figure 4 for fixed fees, the optimal PnL increases with the volume of fundamental flow and decreases with volatility. As is to be expected, the LP performs best in settings with sustained, bidirectional flow and relatively low price volatility.

While we have discussed the dynamics of the optimal AMM fee in detail, an important practical takeaway is that expected PnL is relatively robust around a well-chosen constant fee. As shown in the right panel of Figure 10, setting the AMM fee to roughly 70–80%



Optimal PnL Shortfall Given 15 bps Fee (\$1,000s)

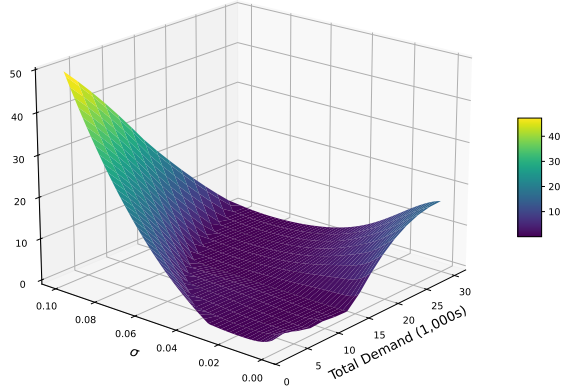


FIGURE 12. Shortfall in expected PnL relative to the optimum from Figure 11 when applying a fixed 15 bps AMM fee, as in Figure 4.

of the CEX fee yields only modest regret across a broad range of volatility and demand levels.<sup>17</sup> Here, regret refers to the shortfall between the expected PnL obtained with a fixed fee and the maximum attainable PnL for each choice of market parameters (i.e., with the optimal fee for those parameters). We visualize this shortfall in Figure 12 by applying a 15 bps AMM fee (approximately 75% of the CEX fee,  $\eta^0 = 20$  bps). We see that along the diagonal of the  $(\sigma, \Delta^B + |\Delta^S|)$  plane, where volatility and demand increase together, the regret from using a constant fee remains minimal. This suggests that in dynamic environments, a fixed fee policy performs particularly well when demand and volatility are positively correlated. On the other hand, in extremely high-volatility environments where the LP would optimally choose to halt trading (i.e., set  $\eta^1 = \infty$ ), the performance loss from maintaining a constant fee becomes substantial. Since cryptocurrency prices do experience such episodes, this regime cannot be neglected.

## 5. EMPIRICAL ANALYSIS

This section evaluates the empirical relevance of our stylized model and examines how fee design affects AMM performance in realistic settings. Our goal is twofold: first, to test whether the model, once calibrated to market data, can replicate key features of observed price and volume dynamics; second, to assess the financial implications of fee optimization, both in simulations and when applied to historical data. To this end, we calibrate the model parameters using minute-level data for the ETH/USDC pair over January 2025, then simulate trading under two fee regimes: the standard Uniswap v2 fee and the fee level predicted by our theoretical optimization. The results show that implementing the optimal fee leads to narrower trading bands and higher execution rates for both arbitrageurs and fundamental traders. From a financial perspective, the AMM’s cumulative PnL improves significantly under the optimal fee, particularly when inventory risk is actively managed. This confirms that fee adjustments can meaningfully enhance AMM profitability, and that

<sup>17</sup>This rule of thumb can change based on the reference CEX fee  $\eta^0$ . See Section 5 for an example where  $\eta^0 \approx 10$  bps.

our modeling framework provides a practical tool to guide fee setting based on empirical data.

**5.1. Data.** Our dataset consists of minute-by-minute records of reserve balances for the ETH/USDC Uniswap v2 pool, extracted via Dune Analytics<sup>18</sup> for the month of January 2025. Using these reserve quantities, we compute the implied DEX price at each timestamp via the constant product formula. The pool applies a fixed fee of 30 basis points and begins the month with reserves of \$23,000,000 and 6,903 ETH. We also obtain minute-level swap volume data for liquidity takers (LTs) in both directions (ETH to USDC and USDC to ETH) over this period.

In parallel, we collect minute-level historical price data for the ETH/USDC pair from Binance, covering the same month.<sup>19</sup> This centralized exchange data serves as a reference price to benchmark and calibrate our model against real market conditions.

**5.2. Calibration.** We calibrate our simulation model to the market data described above for the ETH/USDC pair over the month of January 2025.<sup>20</sup> The central object of interest is the log price ratio process

$$r_t := \log(R_t),$$

computed at each minute from historical data. We construct an empirical histogram of this process and seek to reproduce its distribution through simulation.

For simplicity, we assume that  $\Delta^B = |\Delta^S| =: \bar{\Delta}$ , and that this rate is constant over time. Note that the AMM fee  $\eta^1$  is publicly known. Specifically, we fix  $\eta^1$  to the Uniswap v2 fee for the ETH/USDC pool, i.e.,

$$\eta^1 = 30 \text{ bps.}$$

Recall that for our model we assume that LPs are passive and precommit liquidity to the pool for the *entire* trading horizon. We also treat fees as though they are disbursed directly to the LP. In v2 market data, liquidity is added and withdrawn, and fees contribute to pool liquidity. However, over the horizon we consider pool liquidity does not vary substantially (see Figure 13). Consequently, we fix the liquidity used for calibration to be  $2.3 \cdot 10^7$  USDC and 6904 ETH, which roughly corresponds to the average values of the pool.

This allows us to reduce the calibration problem to three parameters:

- the volatility  $\sigma$  of the CEX price process  $S^0$ ,
- the effective CEX transaction cost  $\eta^0$ ,
- and the arrival rates  $\bar{\Delta}$  of fundamental buyers and sellers, respectively.

Although historical volatility could be used for the value of  $\sigma$ , this leads to an over-estimation of the volatility due to clustering effects, and we rather rely here on a model-implied volatility that allows for a better fit to the price ratio. To estimate the parameters  $(\sigma, \eta^0, \bar{\Delta})$ , we adopt an approach that targets the distribution of the log price ratio between the AMM and the CEX. This focus reflects our earlier finding that price ratio dynamics are central to determining LP profitability. Concretely, we minimize the  $L^2$  distance  $\|\hat{r}_t - r_t\|_2$ , where  $r_t$  is the empirical distribution of the log price ratio, computed from minute-level Binance (CEX) and Uniswap (AMM) prices. The simulated counterpart,  $\hat{r}_t$ , is generated

<sup>18</sup><https://api.dune.com>

<sup>19</sup>Binance price data: <https://data.binance.vision/?prefix=data/spot/monthly/klines/ETHUSDC/1m/>.

<sup>20</sup>We have repeated the same calibration procedure on earlier periods—particularly in 2020 and 2021, when Uniswap v2 enjoyed greater liquidity—and obtained qualitatively similar results. We focus here on a recent window to ensure the relevance of our findings.

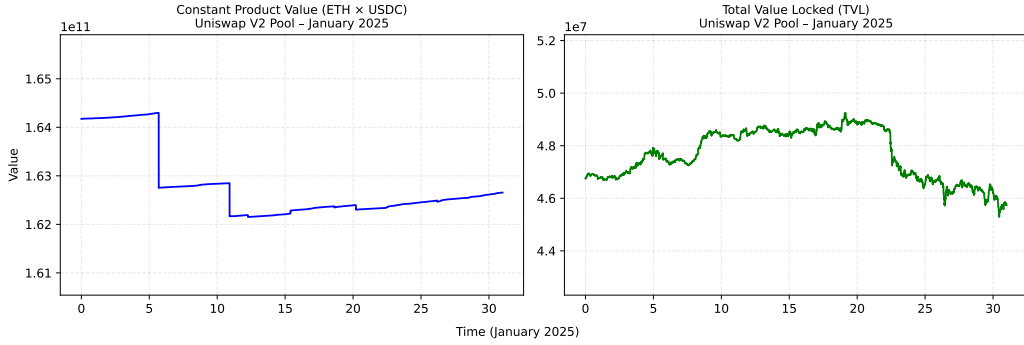


FIGURE 13. Left: evolution of the constant product  $X_t Y_t$  over time in the Uniswap V2 ETH/USDC pool during January 2025. Right: corresponding total value locked (TVL)  $X_t + S_t^1 Y_t = 2X_t$ .

from Monte Carlo simulations using the geometric Brownian motion dynamics (2.1) for the CEX and the stylized AMM trade process detailed in Section 2. The minimization is carried out using a grid search implemented with the `Optuna` optimization library [2]. This method produces consistent estimates for the volatility  $\sigma$  and the effective transaction cost  $\eta^0$ , and accurately captures the empirical shape of the log-ratio distribution, as seen in Figure 14. In particular, this demonstrates that despite its stylized nature, our model can produce parameter values that faithfully capture key features of real-world trading dynamics. The resulting calibrated parameters are reported in Table 2.

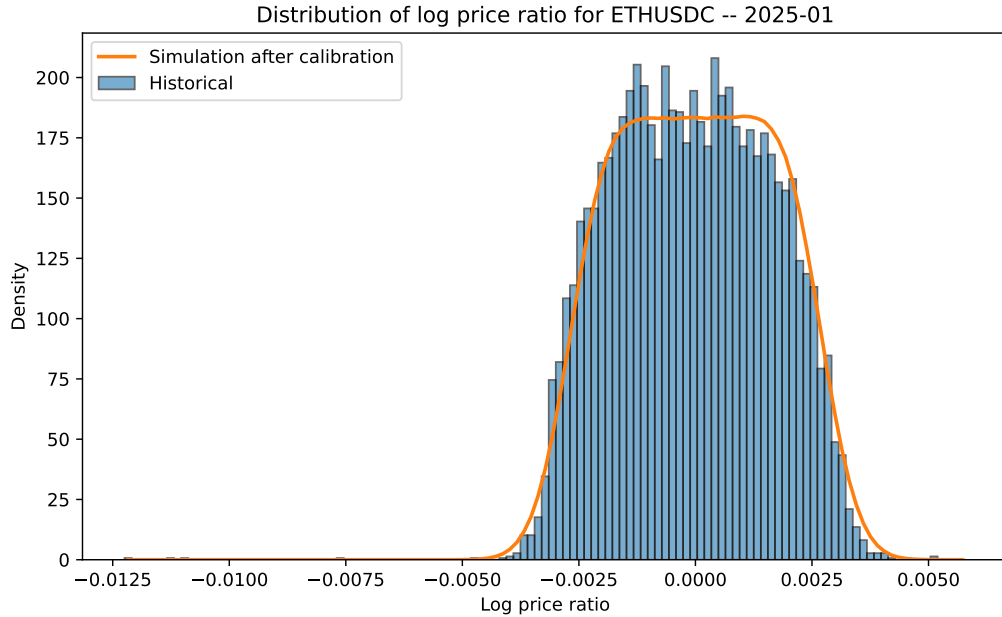


FIGURE 14. Comparison between the historical distribution of the log price ratio (bars) and the simulated distribution after calibration (solid line) for the ETH-USDC pair over January 2025.

TABLE 2. Calibrated parameters with  $\eta^1 = 30$  bps

Parameter	Value	Unit
Buy/sell rate $\bar{\Delta}$	19,068	ETH/day
CEX trading cost $\eta^0$	6.58	basis points (bps)
Daily volatility $\sigma$	2.60%	day <sup>-1/2</sup>

Our model does not explicitly account for gas fees, which represent an additional cost for traders interacting with the AMM. As a result, the value obtained for the CEX trading cost  $\eta^0$  in Table 2 is likely downward-biased. To partially correct for this, we repeat the calibration procedure while adjusting the AMM fee to  $\eta^1 = 35$  bps, thereby approximating the additional gas cost incurred by DEX users. This yields the following estimates, presented in Table 3, which provide a plausible range for  $\eta^0$  that better reflects the all-in trading costs on both venues. Notably, the resulting value for  $\eta^0$  is consistent with observed taker fees on Binance.

TABLE 3. Calibrated parameters with  $\eta^1 = 35$  bps

Parameter	Value	Unit
Buy/sell rate $\bar{\Delta}$	10,338	ETH/day
CEX trading cost $\eta^0$	11.78	basis points (bps)
Daily volatility $\sigma$	2.60%	day <sup>-1/2</sup>

The difference in the estimated arrival rate of fundamental traders  $\bar{\Delta}$  across the two calibrations should not be overinterpreted. High levels of demand tend to produce very similar fits for the distribution of log price ratios when  $\eta^1$  is much larger than  $\eta^0$ , making them statistically hard to distinguish. As such, our estimates are best understood as providing a plausible range of demand intensities consistent with the empirical price ratio distribution.

*Remark 5.1.* As a robustness check, we also performed the calibration by directly using the historical Binance price series for  $S^0$ , instead of simulating it as a geometric Brownian motion. In this setup, the volatility  $\sigma$  is no longer a free parameter, and we calibrate only the effective CEX transaction cost  $\eta^0$  and the net arrival rate  $\bar{\Delta}$  of fundamental traders. We find that this alternative procedure yields similar ranges for both parameters (specifically,  $\bar{\Delta} = 11,684$  ETH/day and  $\eta^0 = 9.87$  bps), reinforcing the robustness of our baseline calibration and suggesting that the geometric Brownian motion assumption for  $S^0$  does not materially affect the identification of key model features.

*Remark 5.2.* While the proposed calibration successfully captures the microstructural dynamics of the AMM, we observe in simulation that the trading volume captured by the AMM is lower than its empirical counterpart (approximately 210 ETH/day versus 750 ETH/day in practice). One possible explanation is the presence of “noise traders” who interact with the AMM independently of relative prices or fees, for idiosyncratic or exogenous reasons. An alternative modeling route is thus to interpret the residual volume gap as arising from such non-strategic order flow. In this interpretation, matching the empirical trading volume would require adding roughly 540 ETH/day of noise-driven trades, which corresponds to

less than 5% of the fundamental volume estimated by our model. This addition has no meaningful impact on the qualitative results that follow, since optimal fee setting remains primarily driven by strategic, incentive-compatible order flow. For clarity of exposition, we omit noise traders from the main analysis, but develop the corresponding extension in Section 6.2. We emphasize that it is expected that realized volume will differ since our model is conservative. Even if we ignore other motivations for trading with the AMM, our simulation logic assumes that traders have perfect knowledge of market prices and can always route optimally, which can fail to hold in practice.

**5.3. Numerical analysis.** We now perform a simulation based on the stylized model and the parameter values estimated in the previous subsection. For the CEX transaction cost, we set  $\eta^0 = 9.18$  bps, which lies at the midpoint of the range identified through the two calibration procedures. Similarly, we set the fundamental demand rate to  $\bar{\Delta} = 14,704$  ETH/day, representing an intermediate value between the two previously estimated demand levels. The simulation is carried out on a minute-by-minute basis over an entire month. Figure 15 reports the expected PnL of liquidity providers as a function of the AMM fee  $\eta^1$ , for various volatility levels in a neighborhood of the calibrated value. We also include a benchmark curve computed using historical CEX prices instead of simulated geometric Brownian motion paths, while keeping the same trade simulation procedure.

The results confirm that the optimal strategy consistently involves undercutting the CEX fee. Moreover, the maximizer of expected PnL remains stable across different volatility values, highlighting the robustness of our framework. Importantly, the fact that the optimal fee remains nearly unchanged when switching from simulated to historical prices suggests that our stylized price model suffices to capture the core tradeoffs involved in fee design. This provides strong support for using simulation-based approaches to optimize AMM parameters, even when abstracting away from complex real-world dynamics such as stochastic volatility and price jumps.

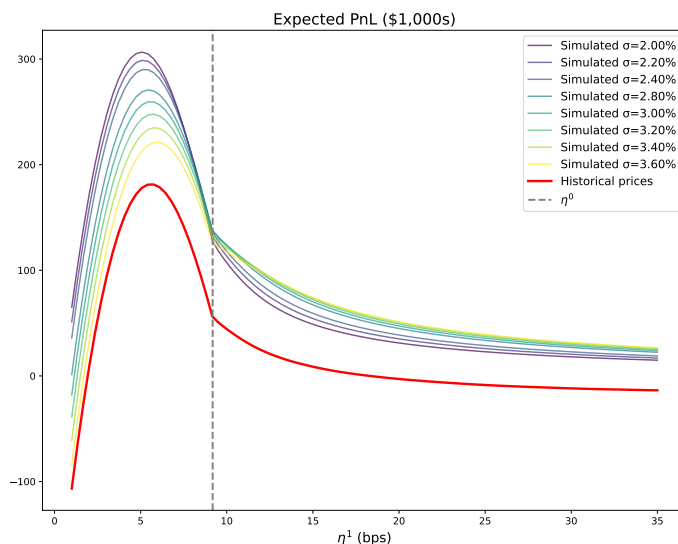


FIGURE 15. Expected PnL of liquidity providers as a function of the AMM fee  $\eta^1$  using historical CEX prices (in red), compared to simulated prices under different volatility levels.

To assess the practical impact of fee design, we evaluate AMM performance on historical price data. Using the volatility estimated in calibration, we identified in the above analysis that the expected PnL is maximized around  $\eta^1 = 5.42$  bps—slightly below the effective CEX fee  $\eta^0$ . As in the earlier analysis of Section 4, this value represents an optimal trade-off between competitiveness and profitability, encouraging volume without unduly sacrificing fee revenue.

To test the real-world relevance of this result, we run two simulations using historical minute-by-minute Binance data:

- In the first, we set  $\eta^1 = 30$  bps, matching the Uniswap v2 fee for ETH/USDC.
- In the second, we rerun the simulation with the optimal fee  $\eta^1 = 5.42$  bps.

Figures 16 and 17 display the results under the standard fee  $\eta^1 = 30$  bps. We observe wide arbitrage bands and sparse trading, reflecting the deterrent effect of high transaction costs. The resulting final PnL, both for the hedged and unhedged strategies, is negative due to limited flow and fewer opportunities to charge trading fees. Echoing the findings of Section 4, PnL deteriorates markedly during the sharp increase in volatility observed between days 18 and 20 in Figure 16.

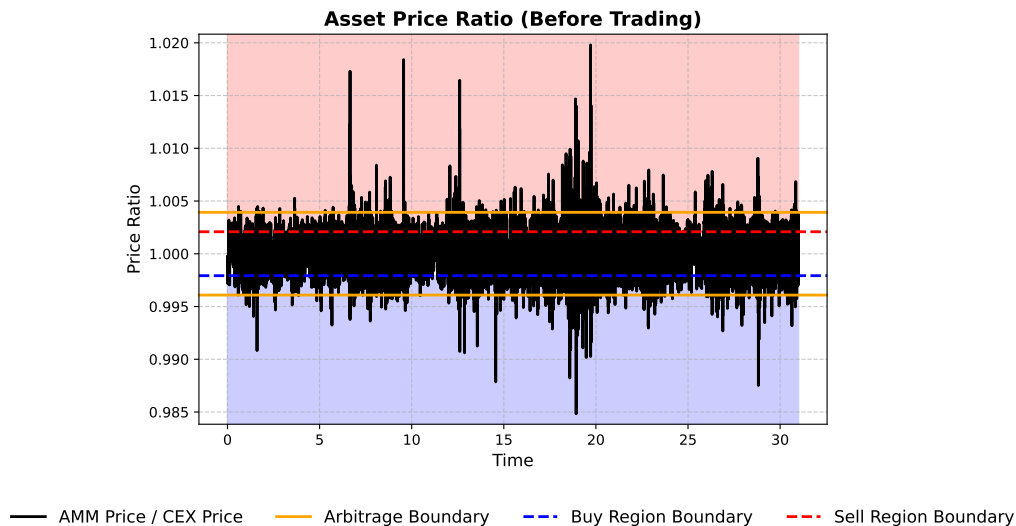


FIGURE 16. Asset price ratio between AMM and CEX prices before trading, based on historical Binance data, with arbitrage and trading region boundaries indicated.

Next, we rerun the same experiment with the optimal fee  $\eta^1 = 5.42$  bps. The resulting dynamics are shown in Figures 18 and 19. With lower fees, we observe a noticeable narrowing of both arbitrage and trading regions. This leads to more frequent arbitrage interventions and significantly increased volume from fundamental traders. Nonetheless, PnL still declines during the day 18 to 20 volatility spike<sup>21</sup> which marks a period when the LP would have benefited from levying a much larger fee.

Overall, the hedged PnL improves substantially and becomes positive under the optimal fee, while the unhedged PnL remains largely unchanged—being mostly driven by the underlying price path. This highlights that fee optimization is most effective when inventory

<sup>21</sup>This coincides with the days leading up to the U.S. presidential inauguration (January 20, 2025).

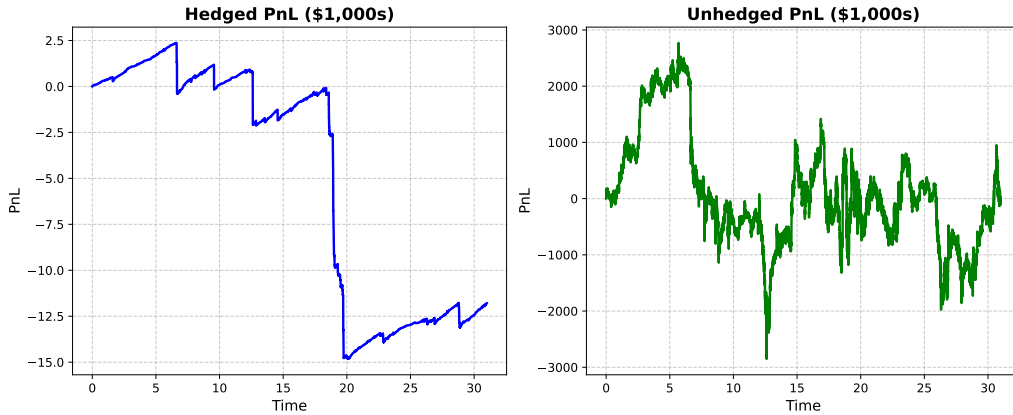


FIGURE 17. Cumulative profit and loss (PnL) for hedged (left) and unhedged (right) AMM strategies over the simulation period using historical data, expressed in thousands of USD, with fee  $\eta^1 = 30$  bps.

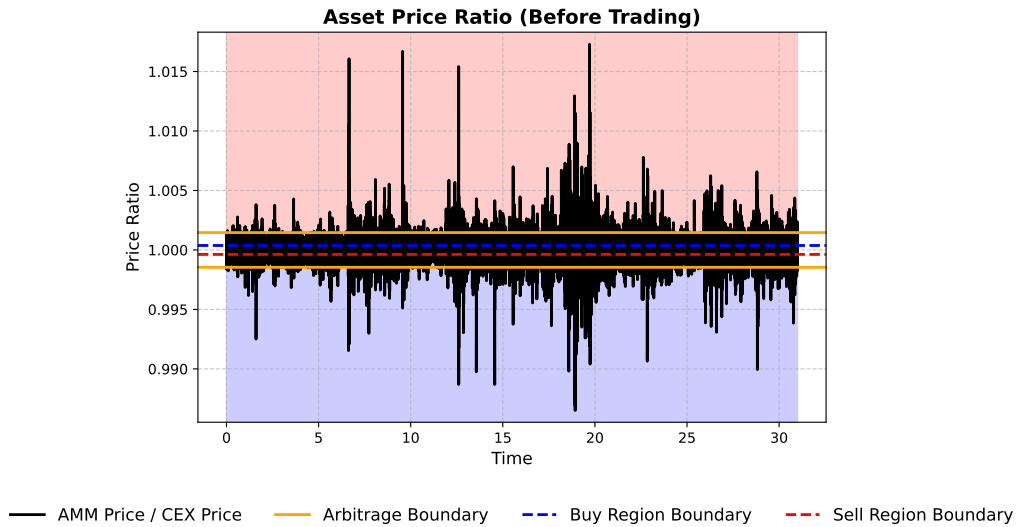


FIGURE 18. Asset price ratio between AMM and CEX prices before trading with optimal DEX fee  $\eta^1 = 5.42$  bps, based on historical Binance data.

risk is actively managed. By lowering its fees, the AMM invites more arbitrage activity, but more importantly it unlocks a much larger share of profitable flow from fundamental traders. The result is a robust increase in PnL.

These findings reinforce a key insight from our earlier analysis: excessive protection against arbitrage can come at the expense of participation from profitable, non-arbitrage trading flows. Striking the right balance is therefore essential. Rather than minimizing arbitrage outright, effective fee design should aim to maximize total value captured by liquidity providers, even if that requires tolerating some arbitrage as part of a broader, healthy market ecosystem. Our empirical results suggest that modestly undercutting the effective CEX fee during stable conditions, combined with significantly increasing fees during

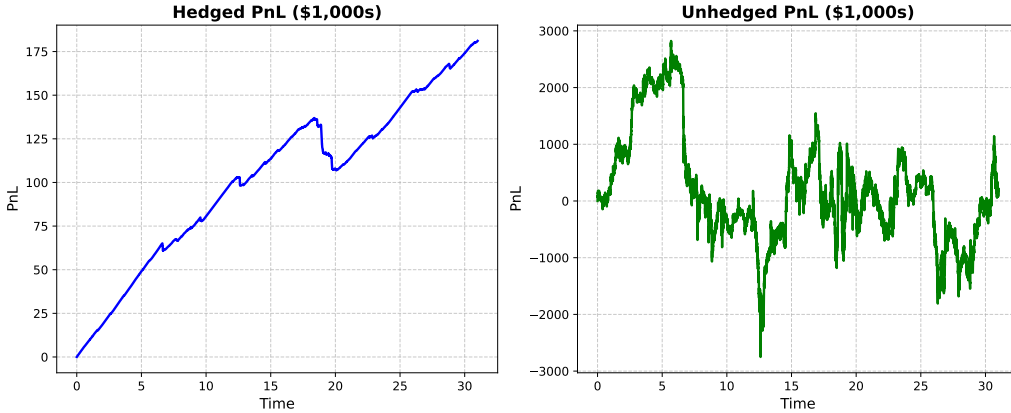


FIGURE 19. Cumulative profit and loss (PnL) for hedged (left) and unhedged (right) AMM strategies over the simulation period with optimal fee  $\eta^1 = 5.42$  bps using historical data.

periods of heightened volatility, provides a practical path to improving LP performance. This principle aligns with the design choices seen in recent protocols such as Uniswap v3, which introduced multiple fee tiers to reflect differing asset profiles, and Uniswap v4, which further enables dynamic fee customization via hooks—underscoring the growing relevance of adaptive fee mechanisms in AMM design.

## 6. EXTENSIONS TO THE MODEL DESIGN

In this section we briefly address several possible extensions of our baseline model. We fix the parameters specified at the beginning of Section 3 as a reference point and assess the impact of each extension in isolation. As we will see, our previous findings are largely robust to perturbations in the model design.

**6.1. Trading Frequency.** As the number of trading periods  $N$  increases—holding total daily fundamental demand constant—the market effectively distributes the same aggregate flow across a greater number of smaller trades. As a result, higher trading frequencies allow the AMM to better absorb fundamental order flow, as each individual trade imposes only a small price impact. This allows the AMM to remain competitive for a larger fraction of the total volume and in turn, enhances LP profitability by increasing the volume captured at each fee level.

This overall performance improvement driven by the trading frequency is illustrated in the left panel of Figure 20. At sufficiently high frequencies, we heuristically observe convergence toward a continuous-time limit. A rigorous analytic treatment of this limiting regime using stochastic process theory will be reported in future work.

**6.2. Noise Traders.** As noted in the Introduction, there likely exist market participants who trade on the DEX even in situations where informed fundamental traders choose not to. We refer to these participants as *noise traders*, though their behavior can stem from a range of plausible exogenous motives. For example, some traders may prefer the DEX due to its reduced compliance burden, seeking to avoid know-your-customer (KYC) requirements on centralized exchanges for privacy or convenience reasons. Moreover, it is likely that many



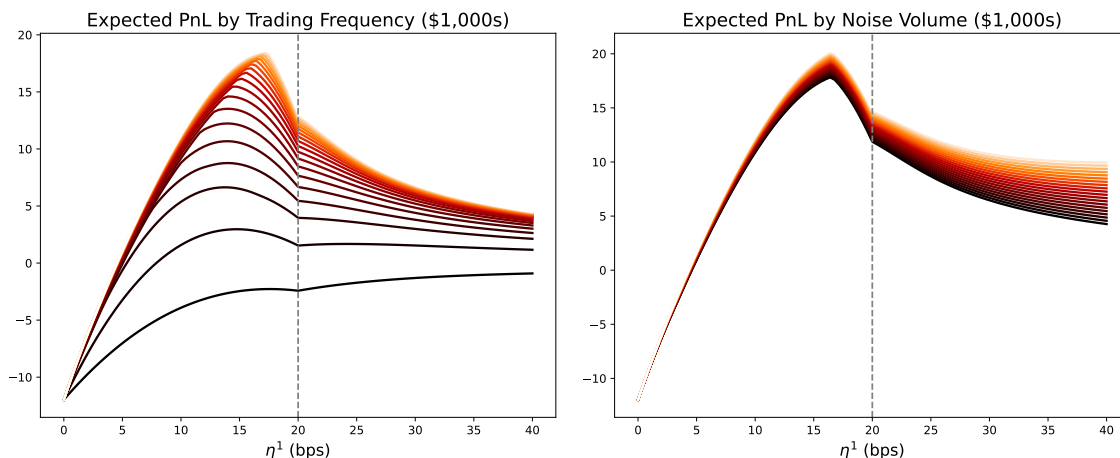


FIGURE 20. (Left) Expected PnL of the LP as the trading frequency  $N$  increases from 100 to 2000. (Right) Expected PnL as the noise volume increases from 0 to 500 units of  $Y$  per day. In both panels the increase in the parameter (i.e.,  $N$ , noise volume) is represented through a color gradient from dark to light.

traders lack perfect information about cross-venue pricing, causing them to frequently route orders in a manner that appears suboptimal ex-post.

There are various ways to model such participants. For simplicity, we consider noise trader flow to be unconditional and insensitive to any reasonable price discrepancies across venues. Specifically, we assume that in each period, a fixed volume of noise trades arrives on the DEX, divided evenly between buy and sell orders. These trades occur after fundamental traders transact, and their symmetric nature ensures they exert no direct influence on the price ratio distribution. Their sole effect is to increase the fee revenue earned by the LP.

Naturally, the assumption of unconditional noise flow is valid only over a restricted fee range. As  $\eta^1 \rightarrow \infty$ , execution costs on the DEX would preclude all participation, including that of noise traders. Absent such a constraint, rational traders would abstain from interacting with the DEX, while noise-driven volume would yield unbounded profits to the LP. Accordingly, we limit noise flow to fee levels that are economically plausible.

The right panel of Figure 20 illustrates the impact of introducing noise trader flow up to 5% of the baseline total unsigned fundamental demand (i.e., 500 units of  $Y$  per day). Even when this flow is completely insensitive to  $\eta^1$ , the qualitative conclusions from Section 4 remain intact for all reasonable fee levels. In particular, while noise flow raises LP profitability across the board, the optimal AMM fee continues to lie strictly below the fee charged on the CEX.

**6.3. Alternative Fees.** We can extend the baseline framework to incorporate more realistic fee structures by introducing two additional parameters: an arbitrageur-specific fee  $\eta^A$  and a hedging fee  $\eta^H$  applied to the LP's CEX trades. These fees capture a more nuanced distinction between market participants. For one, arbitrageurs are often sophisticated actors who may face lower effective fees than other traders. Likewise, LPs typically incur strictly positive costs when rebalancing inventory that *differ* from those faced by fundamental traders. While perhaps non-zero, the hedging fee  $\eta^H$ , which represents the LP's

effective execution cost on the CEX, still ought to be lower than the standard fee  $\eta^0$  due to internal netting, tiered fee schedules, or other preferential arrangements.

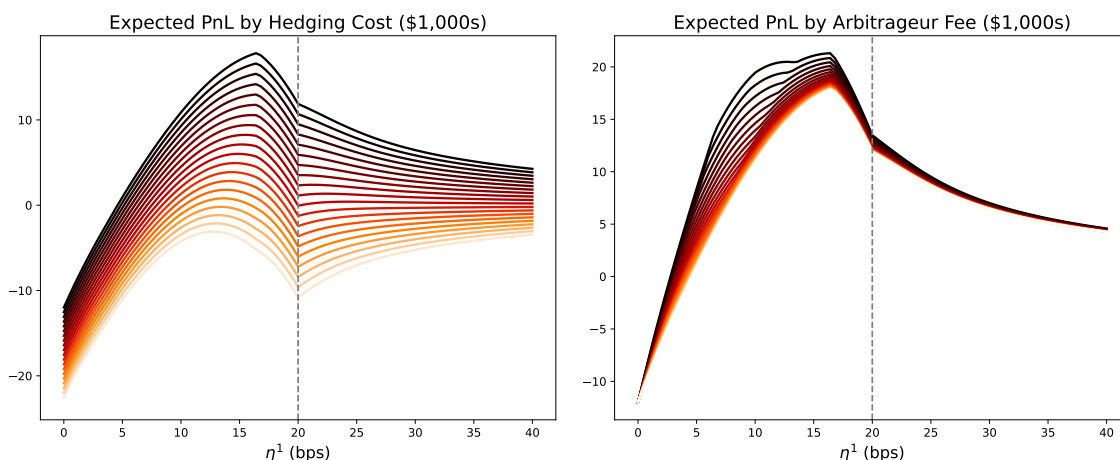


FIGURE 21. (Left) Expected PnL as the hedging cost  $\eta^H$  increases from 0 to  $\eta^0$ . (Right) Expected PnL as the arbitrageur fee  $\eta^A$  increases from 0 to  $\eta^0$ . All of the curves are illustrated on a color gradient from dark to light as  $\eta^H$  and  $\eta^A$  increase.

In view of the tiers for the nominal fees that CEXs levy on their customers' trades based on monthly trading volume, one could also consider a distribution of fundamental trader fees instead of a single value. However, modeling this introduces ambiguity around how to specify trader heterogeneity and so, we do not pursue this latter extension here in detail. In effect, varying fundamental trader fees simply alters the decision thresholds for routing volume to the DEX, and is partly covered by our discussion. Specifically, fundamental traders with a high CEX fee would route almost all their flow to the DEX, making them similar to noise traders (see Section 6.2), whereas fundamental traders with a low CEX fee would route almost all their flow to the CEX and hence become inconsequential for our analysis. In summary, having a spectrum of fundamental trader fees is similar to reducing fundamental demand and adding noise traders.

The introduction of a hedging fee  $\eta^H$  modifies the analysis of Section 2 by increasing the LP's effective cost of inventory adjustments on the CEX. Accounting for this fee, the marginal change in the LP's hedged PnL for a small buy trade ( $\Delta > 0$ ) becomes

$$\text{Change in Hedged PnL} \approx \Delta \cdot S_t^0 [(1 + \eta^1)R_t - (1 + \eta^H)],$$

and for a small sell trade ( $\Delta < 0$ ),

$$\text{Change in Hedged PnL} \approx \Delta \cdot S_t^0 [(1 - \eta^1)R_t - (1 - \eta^H)].$$

The updated profitability thresholds are then given by

$$R_t \geq \frac{1 + \eta^H}{1 + \eta^1} \quad (\text{buy trades}), \quad R_t \leq \frac{1 - \eta^H}{1 - \eta^1} \quad (\text{sell trades})$$

with net effect being that  $\eta^H$  compresses the LP's profit region. As illustrated in Figure 21, since this addition does not change the ratio distribution or volume traded, the additional cost can only decrease the profitability of the LP.

On the other hand, introducing a lower arbitrageur fee  $\eta^A < \eta^0$  pushes the arbitrage boundaries *inwards* towards the profit region. In the extreme case  $\eta^A = 0$  and  $\eta^H = 0$ , the arbitrage and profit boundaries coincide. Thus, in this regime arbitrageurs reflect the price ratio into the region where trading is profitable for the DEX. As demonstrated in Figure 21, this general intuition persists for strictly positive values of  $\eta^A$ , and LP profitability improves as  $\eta^A$  decreases. We collect these observations about the changes to the trading regions of Table 1 in the updated Table 4.

TABLE 4. Generalized Trading and Profitability Thresholds

	Trade Condition	Profit Condition
<b>Fundamental Buyers</b>	$R_t \leq \frac{1 + \eta^0}{1 + \eta^1}$	$R_t \geq \frac{1 + \eta^H}{1 + \eta^1}$
<b>Fundamental Sellers</b>	$R_t \geq \frac{1 - \eta^0}{1 - \eta^1}$	$R_t \leq \frac{1 - \eta^H}{1 - \eta^1}$
<b>Arbitrage Buyers</b>	$R_t \leq \frac{1 - \eta^A}{1 + \eta^1}$	N/A
<b>Arbitrage Sellers</b>	$R_t \geq \frac{1 + \eta^A}{1 - \eta^1}$	N/A

**6.4. Alternative Price Dynamics.** Building on the empirical analysis of Section 5, we can investigate the influence of adding additional characteristics to the price series dynamics. Figure 22 illustrates the sensitivity of the LP’s PnL to prices that exhibit a trend (left) and mean reverting dynamics (right).

We implement the trend by augmenting the reference price dynamics in (2.1) to include a drift parameter  $\mu \in \mathbb{R}$ ,

$$(6.1) \quad \log(S_t^0/S_0^0) = (\mu - \frac{1}{2}\sigma^2)t + \sigma W_t, \quad t \geq 0.$$

Similarly, the mean reverting dynamics are implemented by modeling  $S_t^0$  as the exponential of an Ornstein-Uhlenbeck (OU) process,

$$(6.2) \quad \log(S_t^0/S_0^0) = \int_0^t \kappa(\theta - \log(S_s^0)) ds + \sigma W_t, \quad t \geq 0.$$

Here,  $\kappa > 0$  is the mean reverting force and  $\theta \in \mathbb{R}$  is the reference level. For Figure 22 we fix  $\theta = \log(S_0^0) = \log(3,000)$ .

We see only minor variations of the expected PnL surface for reasonable choices of the new parameters  $\mu$  and  $\kappa$ . Near the optimal fee, the expected (hedged) PnL appears to improve modestly as the trend goes from  $\mu = -4\%$  to  $\mu = 4\%$ . We also see a slight improvement to profitability for fees  $\eta^1 < \eta^0$  when introducing a mean reverting force.<sup>22</sup> Consistent with the analysis of Section 5, we conclude that the general form of the PnL

<sup>22</sup>We note that when the price process is not a martingale, the hedging strategy exhibits a non-zero expected PnL. In Figure 22, we observe a cancellation between two effects: the impact of price dynamics on the unhedged PnL and their effect on the performance of the hedging portfolio. For example, when the price of asset  $Y$  increases, both the pool and the hedging portfolio experience gains since they are long  $Y$ , and these gains partially offset each other. While an LP with perfect knowledge of the price dynamics might opt not to hedge, we do not assume such clairvoyance. To be consistent with our main analysis we focus on the baseline case in which the LP hedges by default.

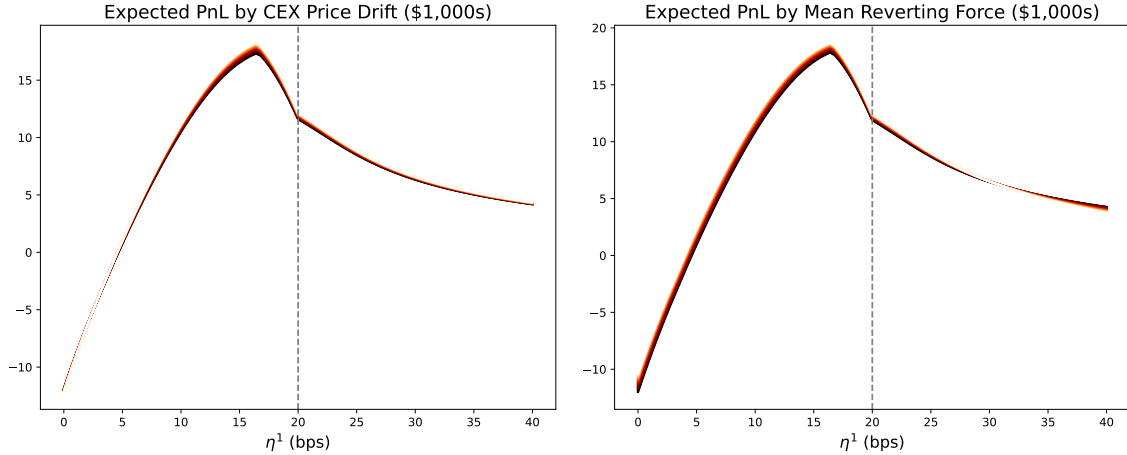


FIGURE 22. (Left) Expected PnL for drift  $\mu \in [-0.04, 0.04]$ . (Right) Expected PnL for mean reverting force  $\kappa \in [0, 100]$ . In both cases the PnL curves are shown on a color gradient from dark to light as  $\mu$  and  $\kappa$  increase.

surface and the overall findings of Section 4 are generally robust to changes in the price dynamics. Importantly, the existence of a maximum in  $\eta^1$  below the (effective) CEX fee persists in this setting.

## 7. CONCLUSION

Using a parsimonious yet flexible reduced-form model of CEX-DEX interaction, we have studied the expected PnL and optimal trading fees for passive liquidity provision to a CPMM as a function of market conditions including volatility and demand. We have also highlighted the mechanisms underlying these dependencies through extensive comparative statics. Our simulation can be calibrated to market data, reproducing realistic price ratio distributions and yielding quantitative, actionable insights.

Our results link the optimal AMM fee level to the trading cost on the CEX and suggest that fees should be competitive with those costs during business-as-usual periods, in particular, potentially lower than the 30 bps fee that was implemented in Uniswap v2 and is still often considered a default for ETH-USDC and comparable pairs. This aligns with the recent popularity of 5 bps Uniswap v3 and v4 pools.<sup>23</sup> In our model, the optimal fee remains remarkably stable throughout normal market conditions. However, our results also suggest that passive liquidity providers need protection during periods of high volatility, such as a high fee that discourages adverse selection on the AMM. Complementary to theoretical studies in toy models, our insights are directly implementable in practice. Specifically, Uniswap v4 hooks could be used to implement a threshold-type dynamic AMM fee which takes two possible values, one that competes with CEX trading costs and a higher rate designed to limit adverse selection in periods of extreme volatility.

<sup>23</sup>For ETH-USDC, 5 bps far dominates 30 bps on Uniswap v4 as of June 30, 2025, with \$130.6M vs. \$5.3M total value locked. Uniswap v3 has \$94M total value locked on 5 bps vs. \$51M on 30 bps. Source: <https://app.uniswap.org/explore/pools/ethereum>

## ACKNOWLEDGEMENTS

The authors thank Patrick Chang, Fayçal Drissi, Ruizhe Jia, Roger Lee, Xin Wan, and numerous conference participants at the Fields Institute and the University of Chicago for helpful discussions. The authors also acknowledge support from a Columbia University CFDT Research Grant and the use of computing resources from Columbia University’s Shared Research Computing Facility project, which is supported by NIH Research Facility Improvement Grant 1G20RR030893-01, and associated funds from the New York State Empire State Development, Division of Science Technology and Innovation (NYSTAR) Contract C090171, both awarded April 15, 2010. S. Campbell is supported in part by an NSERC Fellowship (PDF-599675-2025), and M. Nutz is supported in part by NSF Grants DMS-2407074 and DMS-2106056. J. Milionis’s research is supported in part by NSF awards CNS-2212745, CCF-2332922, CCF-2212233, DMS-2134059, and CCF-1763970, by an Onassis Foundation Scholarship, and an A.G. Leventis educational grant.

## DISCLOSURES

The third author is currently working with blockchain companies not directly involved in AMMs, advising companies on marketplace and incentive design, and has worked with companies involved in creating automated market making protocols, including some referenced in this work. The other authors declare that they do not have any competing interests. Notwithstanding, the ideas and opinions expressed herein are those of the authors, rather than of any of these companies or their affiliates, and should not be construed as or relied upon in any manner as investment, legal, tax, or other advice.

## REFERENCES

- [1] Austin Adams, Ciamac Moallemi, Sara Reynolds, and Dan Robinson. “am-AMM: An Auction-Managed Automated Market Maker”. In: *arXiv preprint arXiv:2403.03367* (2024).
- [2] Takuya Akiba, Shotaro Sano, Toshihiko Yanase, Takeru Ohta, and Masanori Koyama. “Optuna: A next-generation hyperparameter optimization framework”. In: *Proceedings of the 25th ACM SIGKDD International Conference on Knowledge Discovery & Data Mining*. 2019, pp. 2623–2631.
- [3] Algebra Protocol. *ALGEBRA Ecosystem: Decentralized exchange*. 2023. URL: <https://algebra.finance/static/Algebra%20Tech%20Paper-15411d15f8653a81d5f7f574bfe655ad.pdf> (visited on 11/10/2023).
- [4] Guillermo Angeris, Hsien-Tang Kao, Rei Chiang, Charlie Noyes, and Tarun Chitra. “An analysis of Uniswap markets”. In: *arXiv preprint arXiv:1911.03380* (2019).
- [5] Jun Aoyagi and Yuki Ito. “Coexisting Exchange Platforms: Limit Order Books and Automated Market Makers”. SSRN 3808755. 2024.
- [6] Alif Aqsha, Philippe Bergault, and Leandro Sánchez-Betancourt. *Equilibrium Reward for Liquidity Providers in Automated Market Makers*. 2025. arXiv: [2503.22502](https://arxiv.org/abs/2503.22502) [q-fin.TR]. URL: <https://arxiv.org/abs/2503.22502>.
- [7] Leonardo Baggiani, Martin Herdegen, and Leandro Sánchez-Betancourt. *Optimal Dynamic Fees in Automated Market Makers*. 2025. arXiv: [2506.02869](https://arxiv.org/abs/2506.02869) [q-fin.TR]. URL: <https://arxiv.org/abs/2506.02869>.

- [8] Philippe Bergault, Louis Bertucci, David Bouba, and Olivier Guéant. “Automated market makers: mean-variance analysis of LPs payoffs and design of pricing functions”. en. In: *Digital Finance* 6.2 (June 2024), pp. 225–247. ISSN: 2524-6186. DOI: [10.1007/s42521-023-00101-0](https://doi.org/10.1007/s42521-023-00101-0). URL: <https://doi.org/10.1007/s42521-023-00101-0> (visited on 06/17/2025).
- [9] Philippe Bergault, Louis Bertucci, David Bouba, Olivier Guéant, and Julien Guilbert. *Automated Market Making: the case of Pegged Assets*. 2024. arXiv: [2411.08145](https://arxiv.org/abs/2411.08145) [q-fin.TR]. URL: <https://arxiv.org/abs/2411.08145>.
- [10] Philippe Bergault, Louis Bertucci, David Bouba, Olivier Guéant, and Julien Guilbert. *Price-Aware Automated Market Makers: Models Beyond Brownian Prices and Static Liquidity*. 2024. arXiv: [2405.03496](https://arxiv.org/abs/2405.03496) [q-fin.TR]. URL: <https://arxiv.org/abs/2405.03496>.
- [11] Andrea Canidio and Robin Fritsch. “Arbitrageurs’ profits, LVR, and sandwich attacks: batch trading as an AMM design response”. In: *arXiv preprint arXiv:2307.02074* (2023).
- [12] David Cao, Leonid Kogan, Gerry Tsoukalas, and Brett Hemenway Falk. *A Structural Model of Automated Market Making*. Available at SSRN: <https://ssrn.com/abstract=4591447>. 2023.
- [13] Agostino Capponi and Ruizhe Jia. “The adoption of blockchain-based decentralized exchanges”. In: *arXiv preprint arXiv:2103.08842* (2021).
- [14] Álvaro Cartea, Fayçal Drissi, and Marcello Monga. “Decentralized Finance and Automated Market Making: Predictable Loss and Optimal Liquidity Provision”. In: *SIAM Journal on Financial Mathematics* 15.3 (2024), pp. 931–959.
- [15] Álvaro Cartea, Fayçal Drissi, and Marcello Monga. “Predictable losses of liquidity provision in constant function markets and concentrated liquidity markets”. In: *Applied Mathematical Finance* 30.2 (2023), pp. 69–93.
- [16] Cata Labs. *Optimising LP performance part 2: Dynamic fees*. Nov. 2023. URL: <https://blog.catalyst.exchange/optimising-lp-performance-part-2-dynamic-fees/> (visited on 11/10/2023).
- [17] CrocSwap. *Usage of Markout to Calculate LP Profitability in Uniswap V3*. en. 2022. URL: <https://crocswap.medium.com/usage-of-markout-to-calculate-lp-profitability-in-uniswap-v3-e32773b1a88e> (visited on 06/30/2025).
- [18] Atis Elsts. *Conceptualizing Uniswap v3 LP profit and loss*. en. Jan. 2023. URL: <https://atise.medium.com/conceptualizing-uniswap-v3-lp-profit-and-loss-ecbae6e09644> (visited on 06/30/2025).
- [19] Atis Elsts. *Dynamic fees for automated market makers: liquidity, volatility, and collected fees*. en. May 2024. URL: <https://atise.medium.com/dynamic-fees-for-automated-market-makers-liquidity-volatility-and-collected-fees-db211da18d0d>.
- [20] Fenbushi Capital. *Ending LP’s Losing Game: Exploring the Loss-Versus-Rebalancing (LVR) Problem and its Solutions*. Oct. 2023. URL: <https://mirror.xyz/0xbdA5bCe76bF62d97D9C9dF0425CC10079Df1aD75/bW0CccjVC7eoYK0zgmjXFdhWdc8rrUL6Yei-eugF52s> (visited on 06/30/2025).
- [21] Robin Fritsch. “A Note on Optimal Fees for Constant Function Market Makers”. In: *Proceedings of the 2021 ACM CCS Workshop on Decentralized Finance and Security*. 2021, pp. 9–14.

- [22] Lawrence R Glosten and Paul R Milgrom. “Bid, ask and transaction prices in a specialist market with heterogeneously informed traders”. In: *Journal of financial economics* 14.1 (1985), pp. 71–100.
- [23] Joel Hasbrouck, Thomas Rivera, and Fahad Saleh. “An Economic Model of a Decentralized Exchange with Concentrated Liquidity”. In: *Management Science*, forthcoming (2025). URL: <https://doi.org/10.1287/mnsc.2024.04510>.
- [24] Joel Hasbrouck, Thomas Rivera, and Fahad Saleh. “The need for fees at a DEX: How increases in fees can increase DEX trading volume”. In: *Journal of Finance*, forthcoming (2025).
- [25] Xue Dong He, Chen Yang, and Yutian Zhou. *Optimal Design of Automated Market Makers on Decentralized Exchanges*. Available at SSRN: <https://ssrn.com/abstract=4801468>. 2024. URL: <http://dx.doi.org/10.2139/ssrn.4801468>.
- [26] Ariah Klages-Mundt and Steffen Schuldenzucker. *Elliptic Concentrated Liquidity Pool (E-CLP): Technical Overview*. 2022.
- [27] Sorella Labs. *Sorella Labs*. en. 2025. URL: <https://sorellalabs.xyz/writing/a-new-era-of-defi-with-ass> (visited on 08/11/2025).
- [28] Alfred Lehar and Christine A. Parlour. “Decentralized Exchange: The Uniswap Automated Market Maker”. In: *The Journal of Finance* 80.1 (2025), pp. 321–374. DOI: <https://doi.org/10.1111/jofi.13405>. URL: <https://onlinelibrary.wiley.com/doi/abs/10.1111/jofi.13405>.
- [29] LFJ. *Liquidity Book: Primer — LFJ*. 2025. URL: [https://docs.lfj.gg/liquidity/liquidity\\_book-\\_primer\\_6893873](https://docs.lfj.gg/liquidity/liquidity_book-_primer_6893873) (visited on 08/11/2025).
- [30] Jason Milionis, Ciamac C. Moallemi, and Tim Roughgarden. “Extended Abstract: The Effect of Trading Fees on Arbitrage Profits in Automated Market Makers”. In: *Financial Cryptography and Data Security. FC 2023 International Workshops*. Ed. by Aleksander Essex, Shin’ichiro Matsuo, Oksana Kulyk, Lewis Gudgeon, Ariah Klages-Mundt, Daniel Perez, Sam Werner, Andrea Bracciali, and Geoff Goodell. Cham: Springer Nature Switzerland, 2023, pp. 262–265. ISBN: 978-3-031-48806-1.
- [31] Jason Milionis, Ciamac C. Moallemi, Tim Roughgarden, and Anthony Lee Zhang. *Automated Market Making and Loss-Versus-Rebalancing*. Extended abstract published in *Proceedings of the 2022 ACM CCS Workshop on Decentralized Finance and Security, DeFi’22*, <https://dl.acm.org/doi/abs/10.1145/3560832.3563441>. 2022. DOI: [10.48550/ARXIV.2208.06046](https://arxiv.org/abs/2208.06046). URL: <https://arxiv.org/abs/2208.06046>.
- [32] Uniswap. *Dynamic Fees in Uniswap V4*. <https://docs.uniswap.org/contracts/v4/concepts/dynamic-fees>. Accessed: 2024-11-21. 2024.
- [33] Vladislav Volosnikov, Alexander Pimenov, and Vladimir Tikhomirov. *The Impact of Market Conditions and Fee Algorithms on the Design of a Competitive AMM*. Working paper. 2024. URL: <https://algebra.finance/static/the-impact-of-market-conditions-and-fee-algorithms-on-the-design-of-a-competitive-amm.pdf>.

APPENDIX A. PSEUDOCODE FOR SIMULATION

---

**Algorithm 1:** Pseudocode for Simulating Market Dynamics

---

**Input:** Initial reserves  $(X_0, Y_0)$ , CEX prices  $S^0$ , fees  $\eta^0, \eta^1$ , demand sizes  $\Delta^B, \Delta^S$ , time horizon  $T$ , time steps  $N$ , market instances  $M$

**Output:** Reserve paths  $(X_t, Y_t)$ , DEX prices  $S_t^1$ , fee revenues, hedging values  $H_t$

```

1 Initialize market instances and trading flags:
2 for each price path  $j = 1, \dots, M$  do
3   Set reserves:  $(X_0^j, Y_0^j)$  ;
4   Set hedge:  $H_0^j \leftarrow X_0^j + Y_0^j S_0^{0,j}$  ;
5   for each time step  $i = 1, \dots, N$  do
6     Randomly assign  $\text{buyer\_first}_{i,j} \in \{\text{True}, \text{False}\}$  ;
7     Set  $\text{seller\_first}_{i,j} = \neg \text{buyer\_first}_{i,j}$  ;
8 Simulation loop:
9 for each time step  $i = 1, \dots, N$  do
10   for each price path  $j = 1, \dots, M$  do
11     Update hedge portfolio value:  $H_i^j \leftarrow H_{i-1}^j + Y_{i-1}^j \cdot (S_i^{0,j} - S_{i-1}^{0,j})$  ;
12     Arbitrage step:
13     if arbitrage opportunity exists then
14       Compute arbitrage volume  $\Delta_{i,j}^A$  ;
15       Execute arbitrage: update  $(X_i^j, Y_i^j, S_i^{1,j})$  and record fees ;
16     Fundamental trading step:
17     if  $\text{buyer\_first}_{i,j}$  then
18       Compute buy volume on DEX:  $\Delta_{i,j}^{B,DEX}$  ;
19       Execute buy trade: update  $(X_i^j, Y_i^j, S_i^{1,j})$  and record fees ;
20       Compute sell volume on DEX:  $\Delta_{i,j}^{S,DEX}$  ;
21       Execute sell trade: update  $(X_i^j, Y_i^j, S_i^{1,j})$  and record fees ;
22     else if  $\text{seller\_first}_{i,j}$  then
23       Compute sell volume on DEX:  $\Delta_{i,j}^{S,DEX}$  ;
24       Execute sell trade: update  $(X_i^j, Y_i^j, S_i^{1,j})$  and record fees ;
25       Compute buy volume on DEX:  $\Delta_{i,j}^{B,DEX}$  ;
26       Execute buy trade: update  $(X_i^j, Y_i^j, S_i^{1,j})$  and record fees ;

```

---



APPENDIX B. SUMMARY STATISTICS FOR RATIO HISTOGRAMS

TABLE 5. Summary statistics for varying  $\eta^1$  in Figure 6

$\eta^1$ (bps)	5	10	15	20	25
$\mathbb{E}[\text{profit}]$ (\$)	946.51	10881.14	17031.02	11877.55	8682.79
$\mathbb{E}[\text{fees}]$ (\$)	12937.55	22872.52	29022.89	23869.56	20672.64
$\mathbb{E}[\text{volume}]$	8626.36	7625.19	6450.42	3979.41	2757.35
$\mathbb{P}(\text{profit})$	24.74%	51.44%	72.89%	85.93%	91.17%
$\mathbb{P}(\text{buy-sell})$	66.79%	51.44%	29.15%	0.00%	0.00%
$\mathbb{P}(\text{arb})$	9.35%	3.72%	1.59%	0.77%	0.48%

TABLE 6. Summary statistics for varying  $\eta^0$  in Figure 6

$\eta^0$ (bps)	0	5	20	35	60
$\mathbb{E}[\text{profit}]$ (\$)	-3482.90	-1576.77	17031.02	26137.29	29612.52
$\mathbb{E}[\text{fees}]$ (\$)	8507.31	10417.23	29022.89	38116.95	41543.90
$\mathbb{E}[\text{volume}]$	1891.54	2316.01	6450.42	8471.36	9233.20
$\mathbb{P}(\text{profit})$	64.77%	71.42%	72.89%	55.46%	29.95%
$\mathbb{P}(\text{buy-sell})$	0.00%	0.00%	29.15%	70.03%	84.97%
$\mathbb{P}(\text{arb})$	35.19%	14.73%	1.59%	0.64%	0.33%

TABLE 7. Summary statistics for varying  $\sigma$  in Figure 6

$\sigma$	2.50%	3.25%	4.00%	4.75%	5.50%
$\mathbb{E}[\text{profit}]$ (\$)	27382.31	22319.82	17031.02	11676.99	6223.08
$\mathbb{E}[\text{fees}]$ (\$)	32068.21	30237.50	29022.89	28585.86	28891.86
$\mathbb{E}[\text{volume}]$	7126.94	6720.19	6450.42	6353.62	6422.21
$\mathbb{P}(\text{profit})$	94.00%	83.94%	72.89%	63.39%	55.97%
$\mathbb{P}(\text{buy-sell})$	47.45%	36.71%	29.15%	23.97%	20.43%
$\mathbb{P}(\text{arb})$	0.01%	0.29%	1.59%	4.17%	7.59%

TABLE 8. Summary statistics for varying demand in Figure 6

$\Delta^B =  \Delta^S $	1000	3000	5000	7000	9000
$\mathbb{E}[\text{profit}]$ (\$)	-4133.82	5570.90	17031.02	28459.36	36430.06
$\mathbb{E}[\text{fees}]$ (\$)	7836.39	17556.25	29022.89	40453.67	48426.54
$\mathbb{E}[\text{volume}]$	1742.01	3902.03	6450.42	8991.11	10764.58
$\mathbb{P}(\text{profit})$	46.80%	63.50%	72.89%	76.30%	78.27%
$\mathbb{P}(\text{buy-sell})$	16.51%	24.31%	29.15%	30.82%	31.90%
$\mathbb{P}(\text{arb})$	11.62%	4.27%	1.59%	0.77%	0.44%

APPENDIX C. INFINITE DEMAND AND  $\sigma = 0$  APPROXIMATION

Since demand is infinite and purchases/sales occur only at the sell/buy boundaries, respectively, we have the following volumes (when non-zero)

$$\Delta_t^{B,DEX} = Y_t \left( 1 - \sqrt{\frac{(1 - \eta^0)(1 + \eta^1)}{(1 - \eta^1)(1 + \eta^0)}} \right), \quad \Delta_t^{S,DEX} = Y_t \left( 1 - \sqrt{\frac{(1 + \eta^0)(1 - \eta^1)}{(1 + \eta^1)(1 - \eta^0)}} \right).$$

The corresponding fee revenue collected by the LP is

$$\text{Buy Revenue} = \eta^1 P_t [\Delta_t^{B,DEX}] \Delta_t^{B,DEX}, \quad \text{Sell Revenue} = \eta^1 P_t [\Delta_t^{S,DEX}] \left| \Delta_t^{S,DEX} \right|,$$

and the expected fee revenue per period (when initializing the price ratio at either the buy or sell boundary) is thus given by

$$\mathbb{E} [\text{Fee Revenue per period}] = \mathbb{E} [\text{Buy Revenue} + \text{Sell Revenue}].$$

Substituting the trade expressions and simplifying (using that we pick up approximately 75% of a round trip and that  $X_t \approx X_0$ ) yields

$$(C.1) \quad \frac{1}{N} \mathbb{E} [\text{Fee Revenue}] \approx \frac{3}{4} X_0 \eta^1 \left[ \sqrt{\frac{(1 + \eta^0)(1 - \eta^1)}{(1 + \eta^1)(1 - \eta^0)}} - \sqrt{\frac{(1 - \eta^0)(1 + \eta^1)}{(1 - \eta^1)(1 + \eta^0)}} \right].$$

Expanding (C.1) to second order in  $\eta^0$  and  $\eta^1$  gives the expression reported in Section 4.2. An illustration of the approximation accuracy of (C.1) for various demands is given in Figure 23.

As an aside, we recall the breakdown in monotonicity of the optimal fee with respect to demand observed in Figure 10 of Section 4. Figure 23 exposes the precise mechanism by which monotonicity fails: the curve's maximum translates abruptly from left to right at an intermediate demand level.

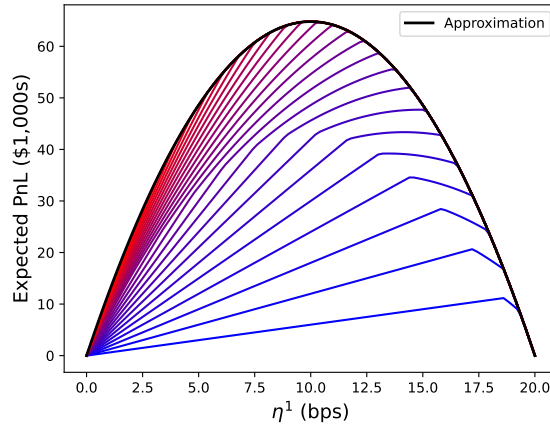


FIGURE 23. Illustration of the infinite demand approximation in (C.1) (black curve) for parameters  $\sigma = 0$  and  $\eta^0 = 20\text{bps}$ . The expected PnL curves for various demand levels  $\Delta^B = |\Delta^S| \in \{1000, 2000, \dots, 25000\}$  are provided on an increasing gradient from blue to red.

DEPT. OF STATISTICS, COLUMBIA UNIVERSITY  
*Email address:* `sc5314@columbia.edu`

CEREMADE, UNIVERSITÉ PARIS DAUPHINE-PSL  
*Email address:* `bergault@ceremade.dauphine.fr`

DEPT. OF COMPUTER SCIENCE, COLUMBIA UNIVERSITY AND CATEGORY LABS  
*Email address:* `jm@cs.columbia.edu`

DEPTS. OF STATISTICS AND MATHEMATICS, COLUMBIA UNIVERSITY  
*Email address:* `mnutz@columbia.edu`